Quantum simulators consisting of lattice-confined sodium antiferromagnetic and rubidium ferromagnetic spinor condensates

Yingmei Liu & Members and Collaborators of

Ultra-cold Quantum Simulator Group, Oklahoma State University

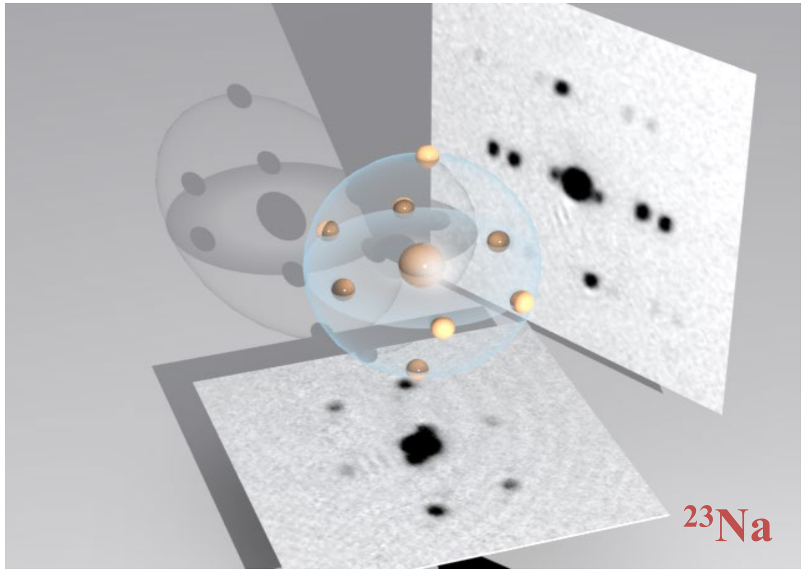

3D monoclinic lattices

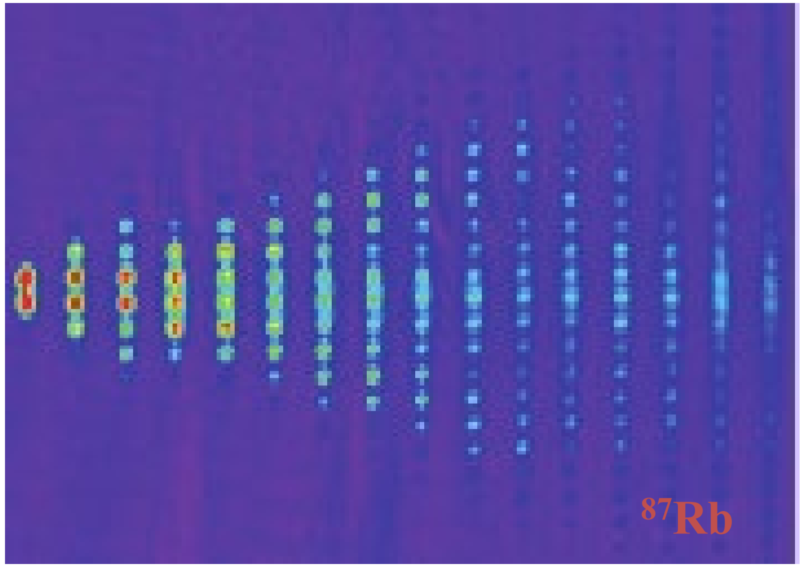

Discrete-time quantum walks

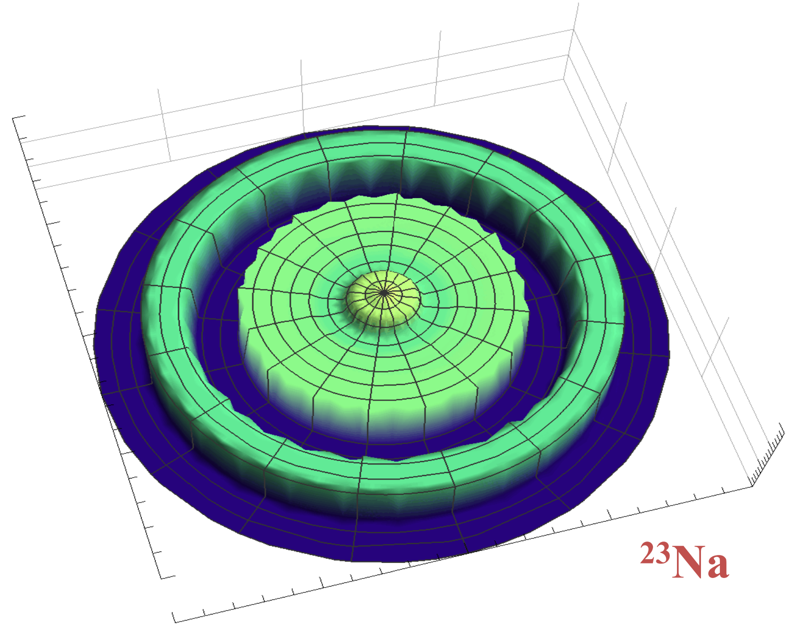

Spatial dynamics in cubic lattices

F=1 spinor BECs: multi-component BECs with spin-dependent interactions

Interaction energy in the collision:

$$V_{int} = \left(\boxed{c_0} + \boxed{c_2 \vec{F}_1 \cdot \vec{F}_2} \right) \delta(\vec{r}_1 - \vec{r}_2)$$

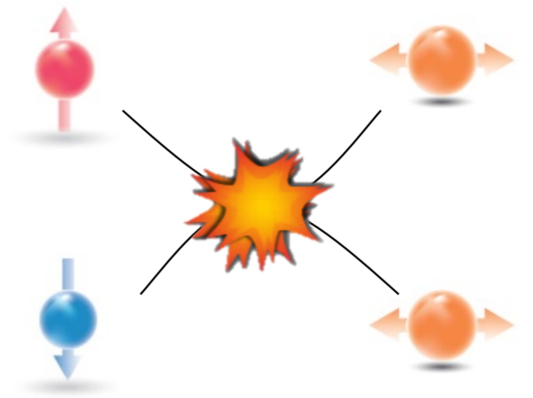

When $F_n = 1$, the total spin $f = F_1 + F_2 = 0$ or 2

Spin-independent

$$c_0 = \frac{4\pi\hbar^2}{M} \frac{2a_{f=2} + a_{f=0}}{3}$$

Spin-dependent

$$c_2 = \frac{4\pi\hbar^2}{M} \frac{a_{f=2} - a_{f=0}}{3}$$

a_f : s-wave scattering length

"Ferromagnetic" (^{87}Rb)

$c_2 < 0$

"Antiferromagnetic" (^{23}Na)

$c_2 > 0$

The lowest energy states:

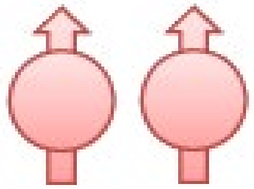

(f = 2)

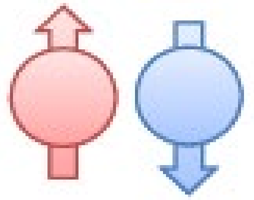

(f = 0)

F=1 spinor BEC: Coherent Spin-Changing Collisions

The only interesting collisions

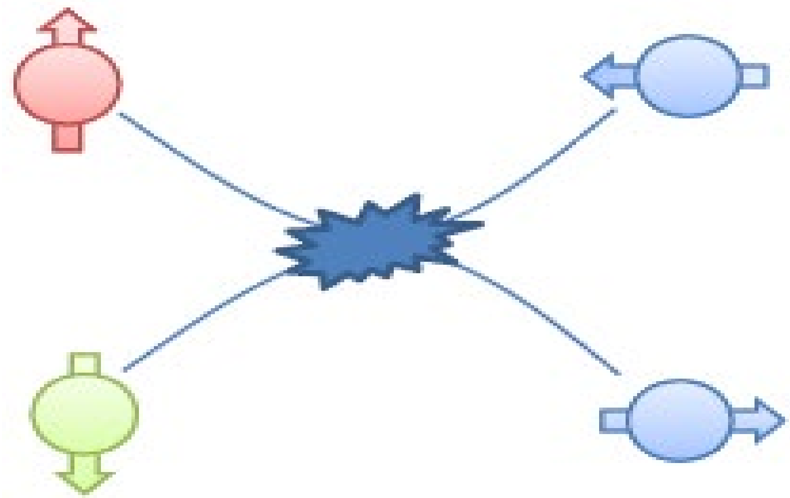

$$|+1\rangle\,|-1\rangle \Leftrightarrow |0\rangle\,|0\rangle$$

Two conservations in the collision:

1. Magnetization: $m = \rho_{+1} - \rho_{-1}$
2. Total atoms: $\rho_{+1} + \rho_0 + \rho_{-1} = 1$

ρ_i : the fractional population of a spin state

Because no observed spin domains

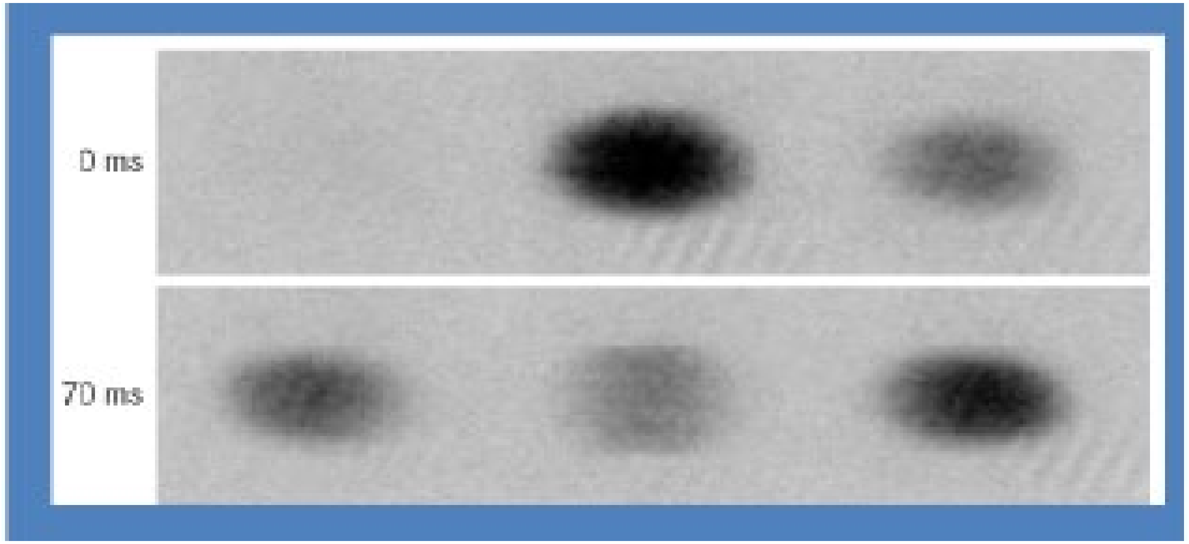

Single Spatial Mode Approximation
(SMA)

$$\psi(\mathbf{r},t) = \sqrt{n(\mathbf{r})}\begin{pmatrix} \sqrt{\rho_{-1}(t)}e^{i\theta_{-1}(t)} \\ \sqrt{\rho_0(t)}e^{i\theta_0(t)} \\ \sqrt{\rho_{+1}(t)}e^{i\theta_{+1}(t)} \end{pmatrix}$$

F=1 spinor BEC : when a magnetic field is applied

For a single particle

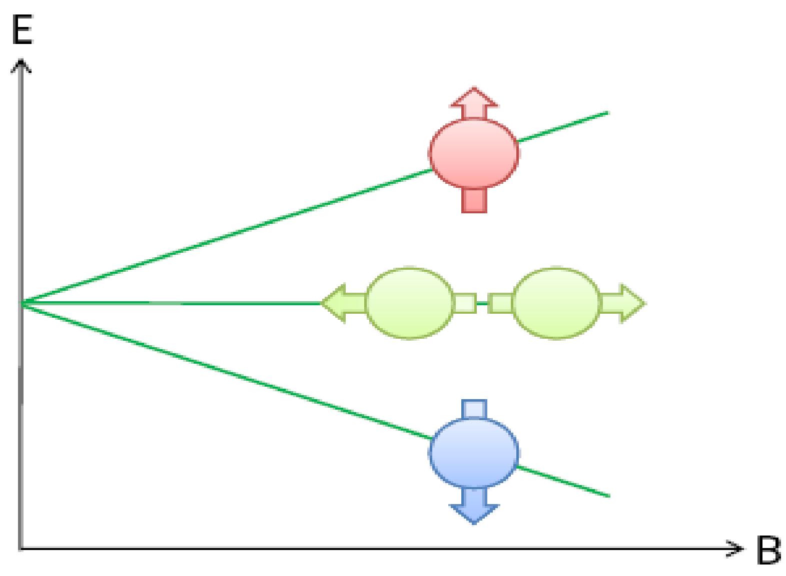

In the collision: two particles

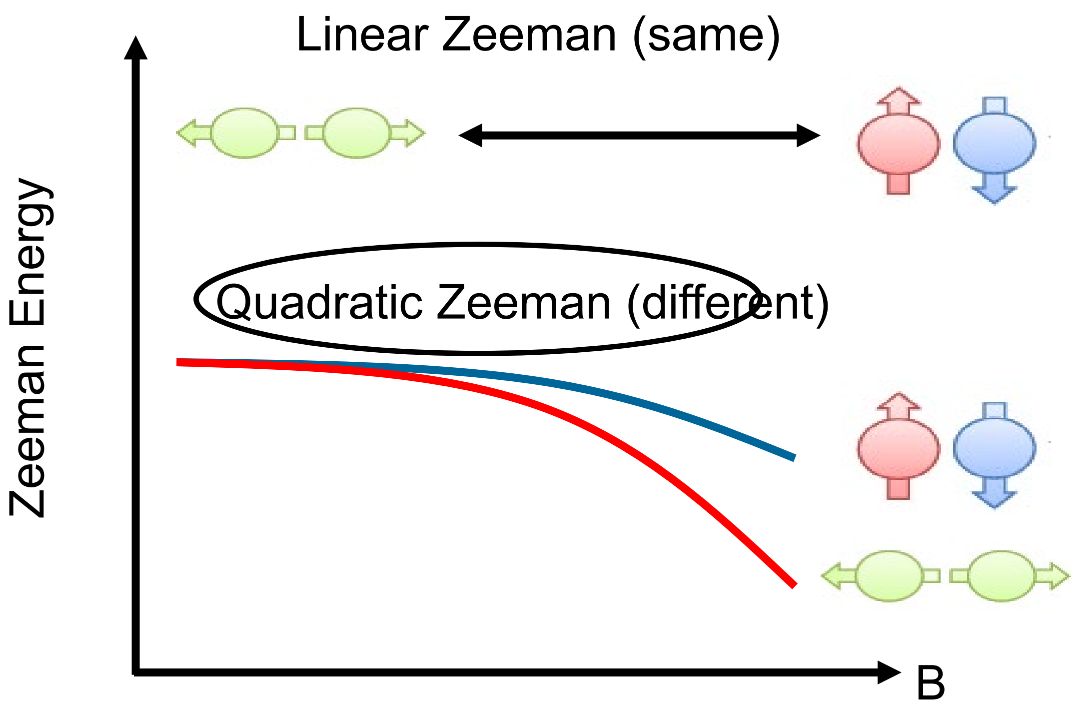

Hamiltonian of F=1 spinor BECs in free space derived from SMA

$$E = \underbrace{q_{\mathrm{net}}(1-\rho_0)}_{\text{Quadratic Zeeman term}} + \underbrace{c\rho_0\left[(1-\rho_0) + \sqrt{(1-\rho_0)^2 - m^2}\cos\theta\right]}_{\text{Spin dependent term}}$$

Two variables remain: ρ_0 and ϑ

$$q_{\mathrm{net}} = q_{\mathrm{B}} + q_{\mathrm{M}} \qquad c = c_2\langle n\rangle \qquad m = \rho_+ - \rho_- \qquad \theta = \theta_+ + \theta_- - 2\theta_0$$

3D highly-programmable spinor quantum simulators realized in our lab

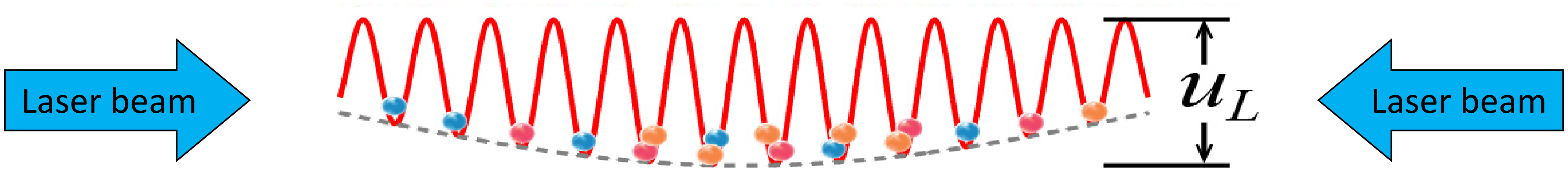

Cold atoms ~ 50 nK

2D optical lattices

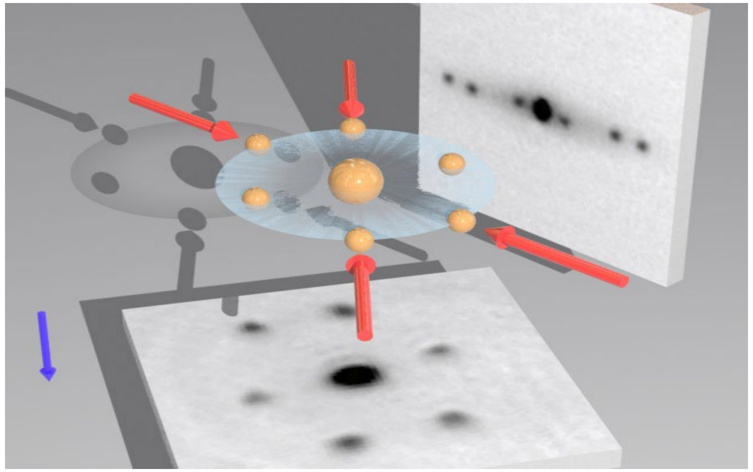

3D cubic lattices

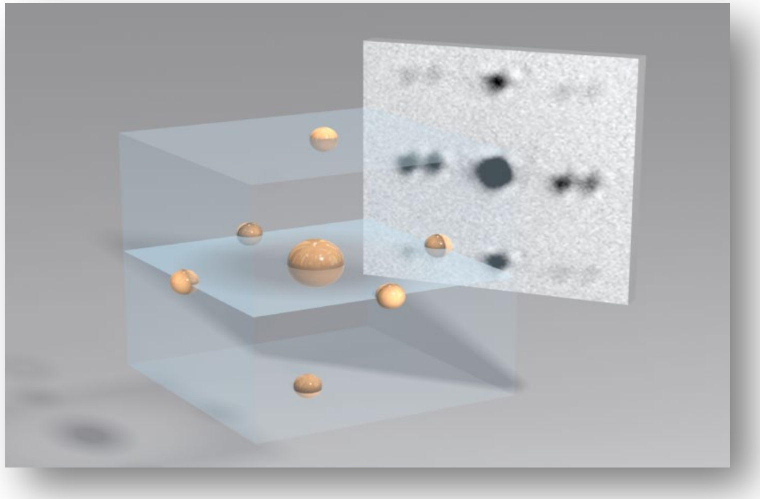

3D monoclinic lattices

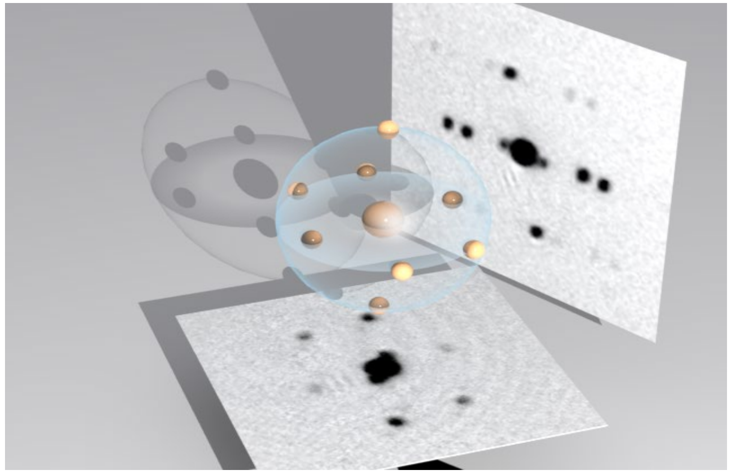

F=1 spinor BECs in Optical Lattices

Bose-Hubbard model

$$H = -\overbrace{J\sum_{<i,j>,k} a^{\dagger}_{ik}a_{jk}}^{\text{Hopping term}} + \overbrace{U_0\sum_{i} n_i(n_i-1)/2}^{\text{Spin independent term}} - \mu\sum_{i} n_i$$

$$+\underbrace{U_2\sum_{i}(F_i\cdot F_i-2n_i)/2}_{\text{Spin dependent term}} + \underbrace{q_{\text{net}}\sum_{i,k} k^2 n_{ik}}_{\text{Quadratic Zeeman term}} - \mu_m\sum_{i,k} k n_{ik}$$

a_{ik}: annihilation operator of a boson in magnetic sublevel k and lattice site i

$$n_i = \sum_{k} a^{\dagger}_{ik}a_{ik}$$

μ: chemical potential

Spinor BECs in optical lattices: 3D Programmable quantum simulator with many tunable parameters, such as temperature, spin, density, and dimensionality

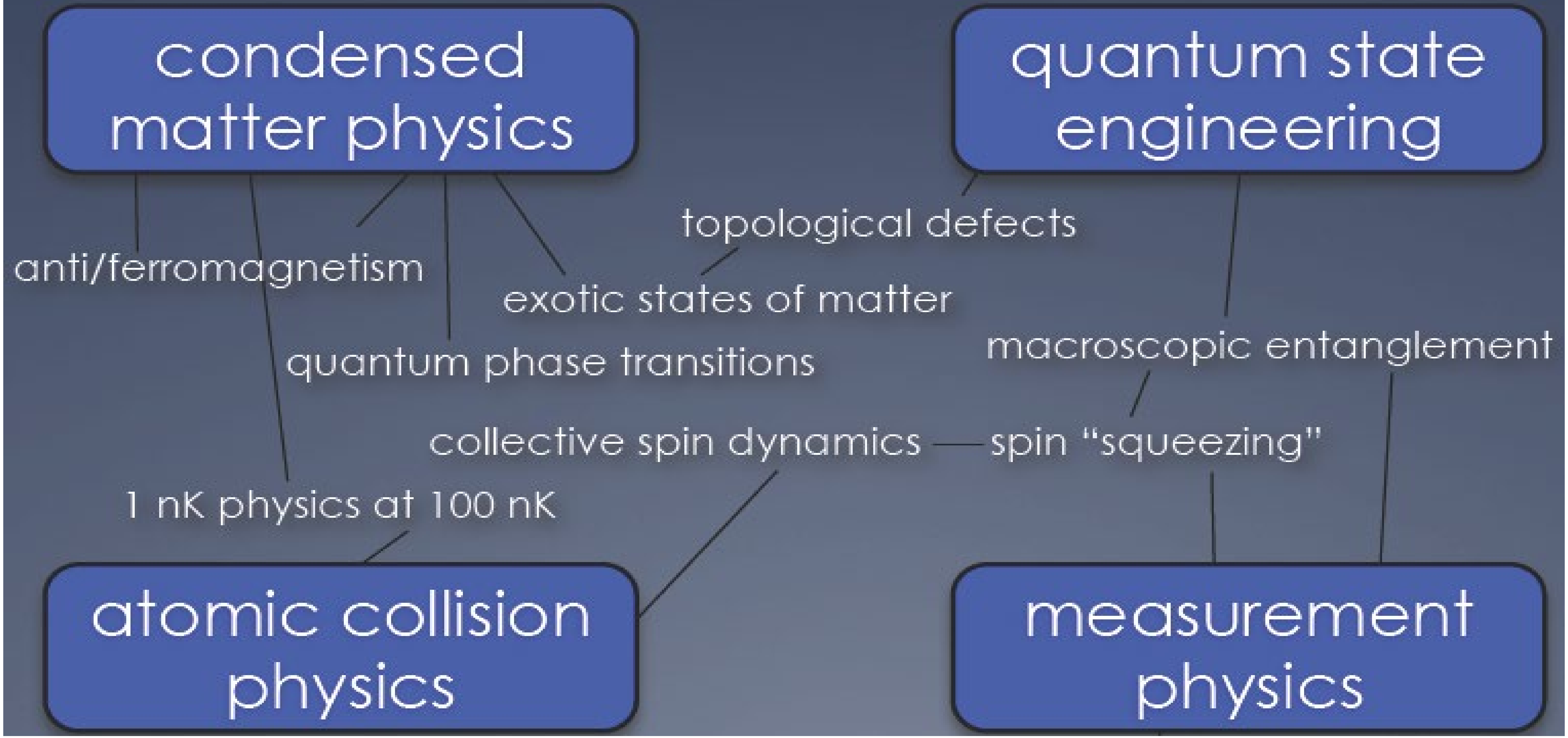

Quantum quench → Nonequilibrium dynamics

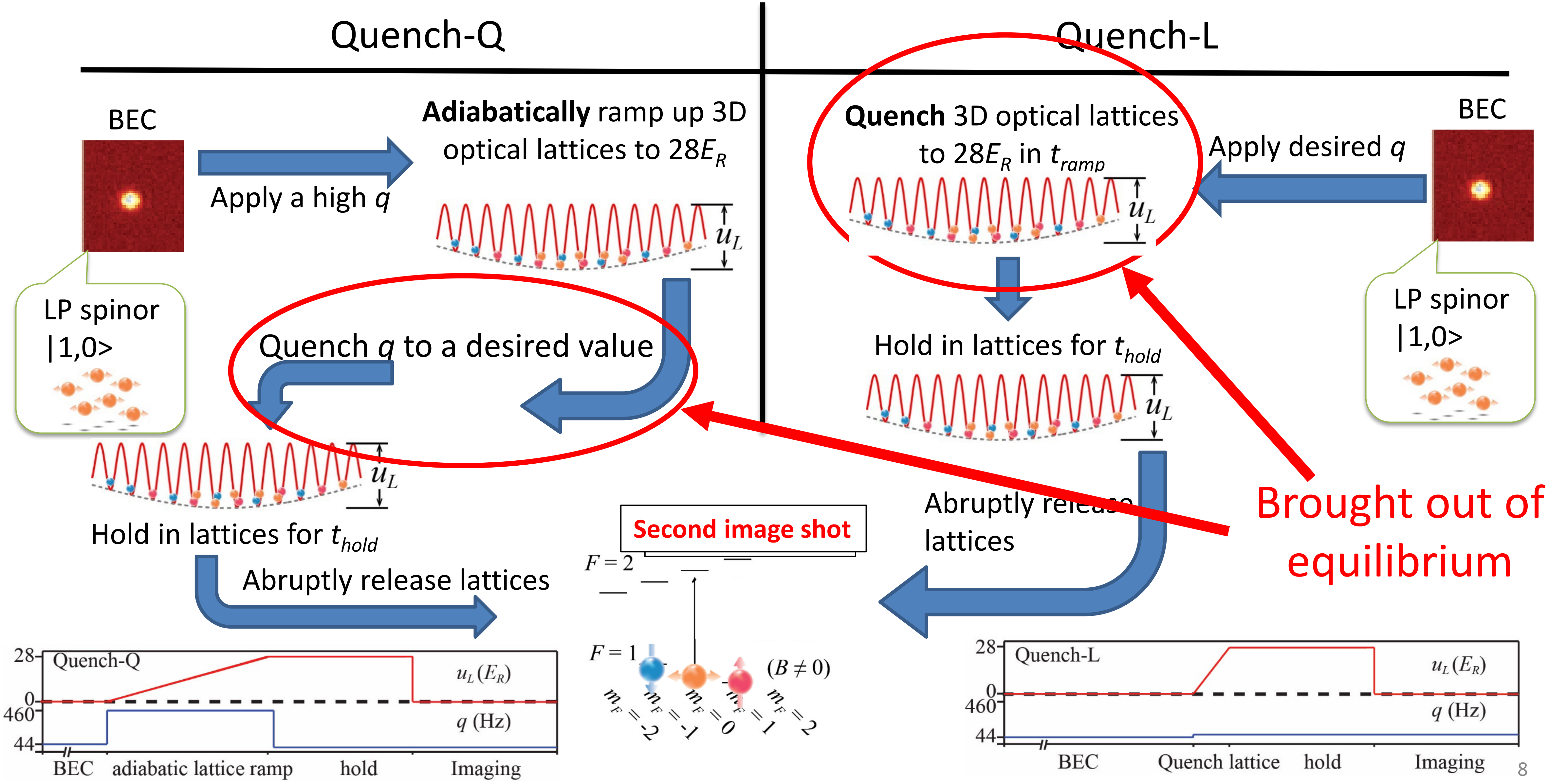

Observation of few-body nonequilibrium spin dynamics

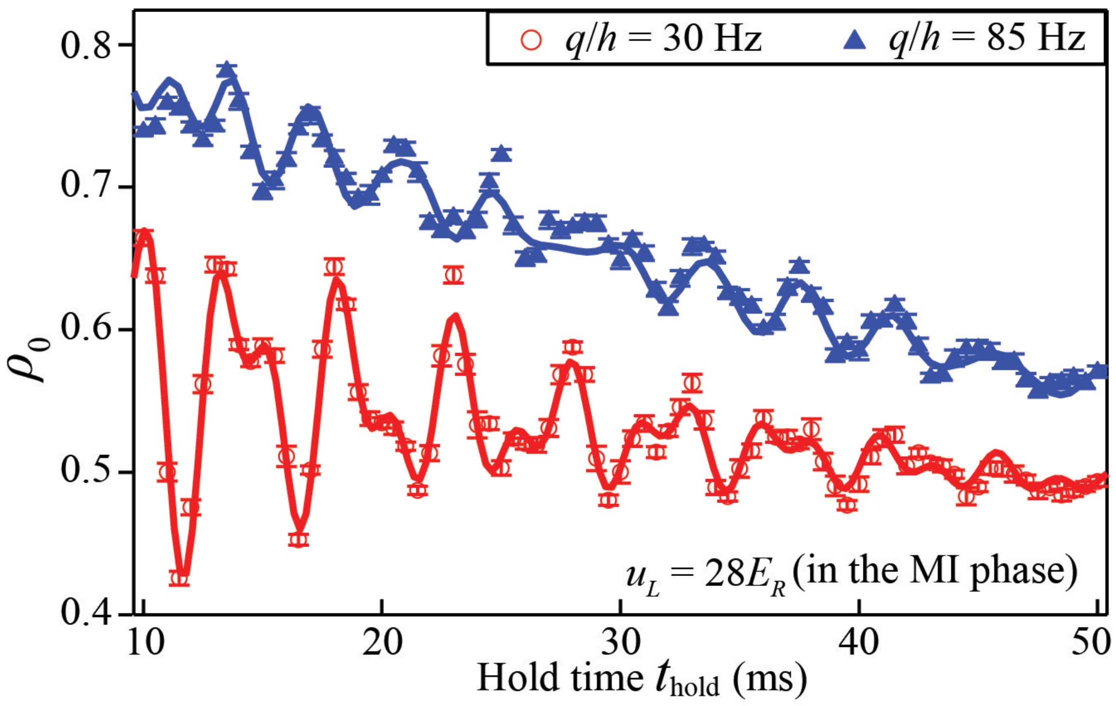

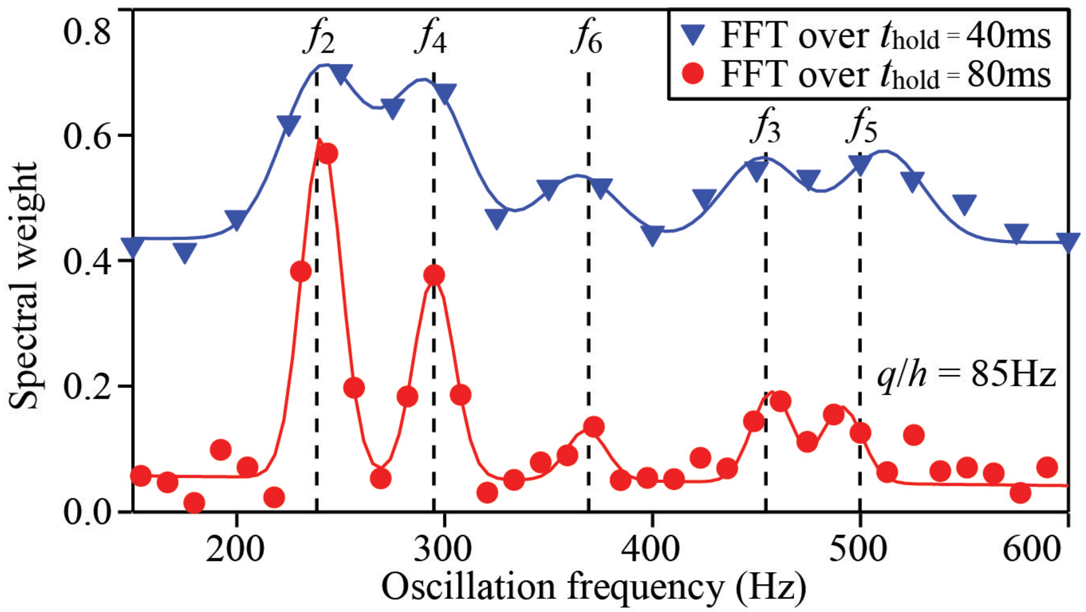

The underlying physics is revealed by a fast Fourier Transform (FFT)

Predicted Energy Gap in Deep Lattices

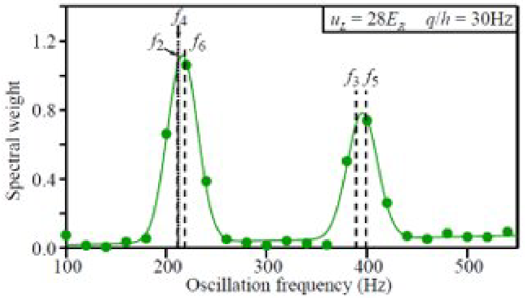

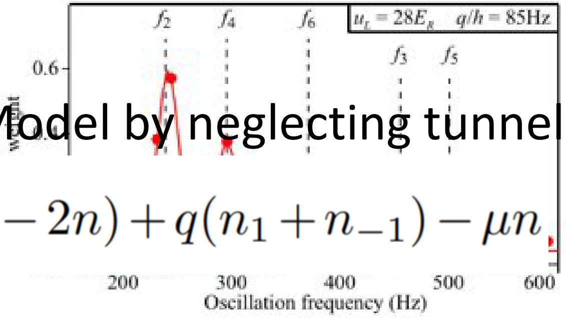

rd Model by neglecting tunneling

$(\vec{S}^2 - 2n) + q(n_1 + n_{-1}) - \mu n$

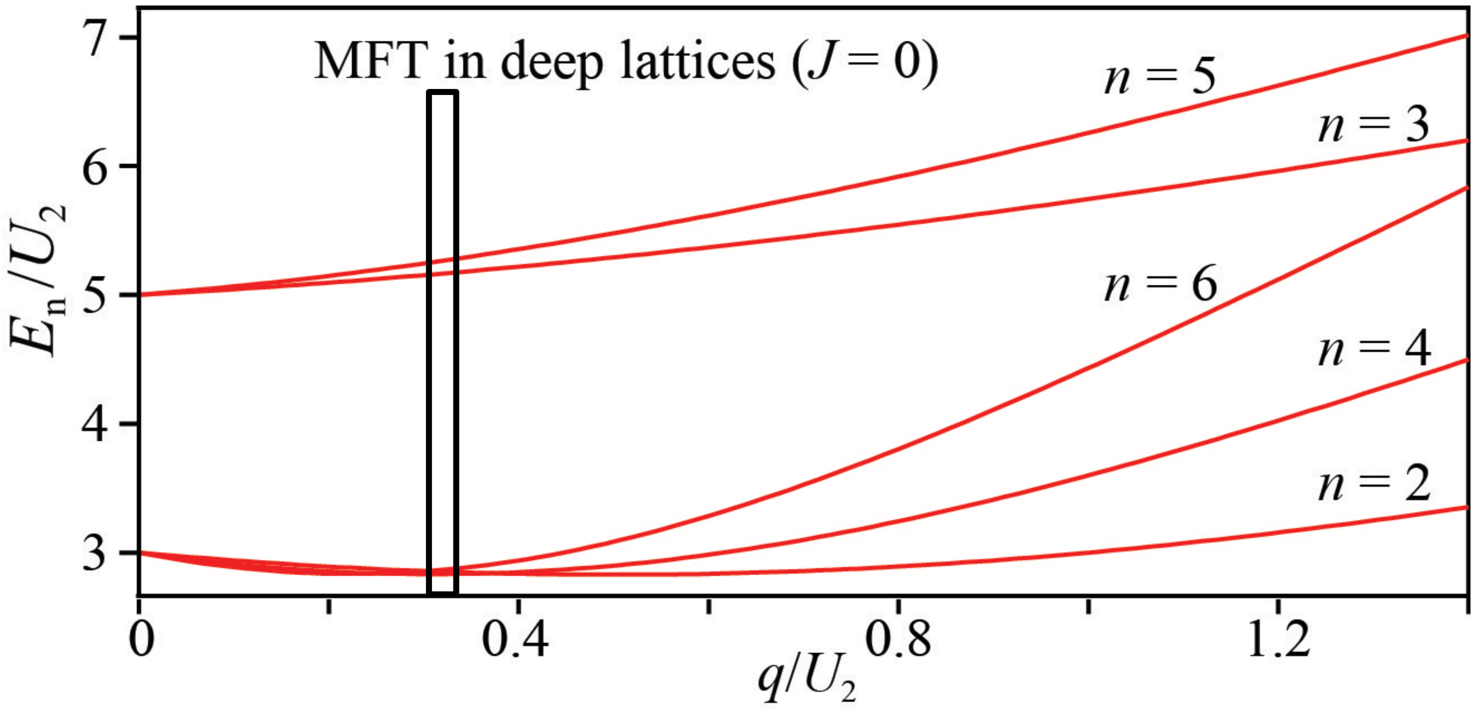

S: spin operator

q: net quadratic Zeeman energy

μ: chemical potential

n: total atom number in each lattice site

E_n is the energy gap between the ground state and the first excited state at a given n

$$f_n = E_n/h$$

$$f_2 = U_2\sqrt{9 - 4(q/U_2) + 4(q/U_2)^2}/h$$

$$f_3 = U_2\sqrt{25 + 4(q/U_2) + 4(q/U_2)^2}/h$$

Utilize the FFT spectrum to extract the number distribution

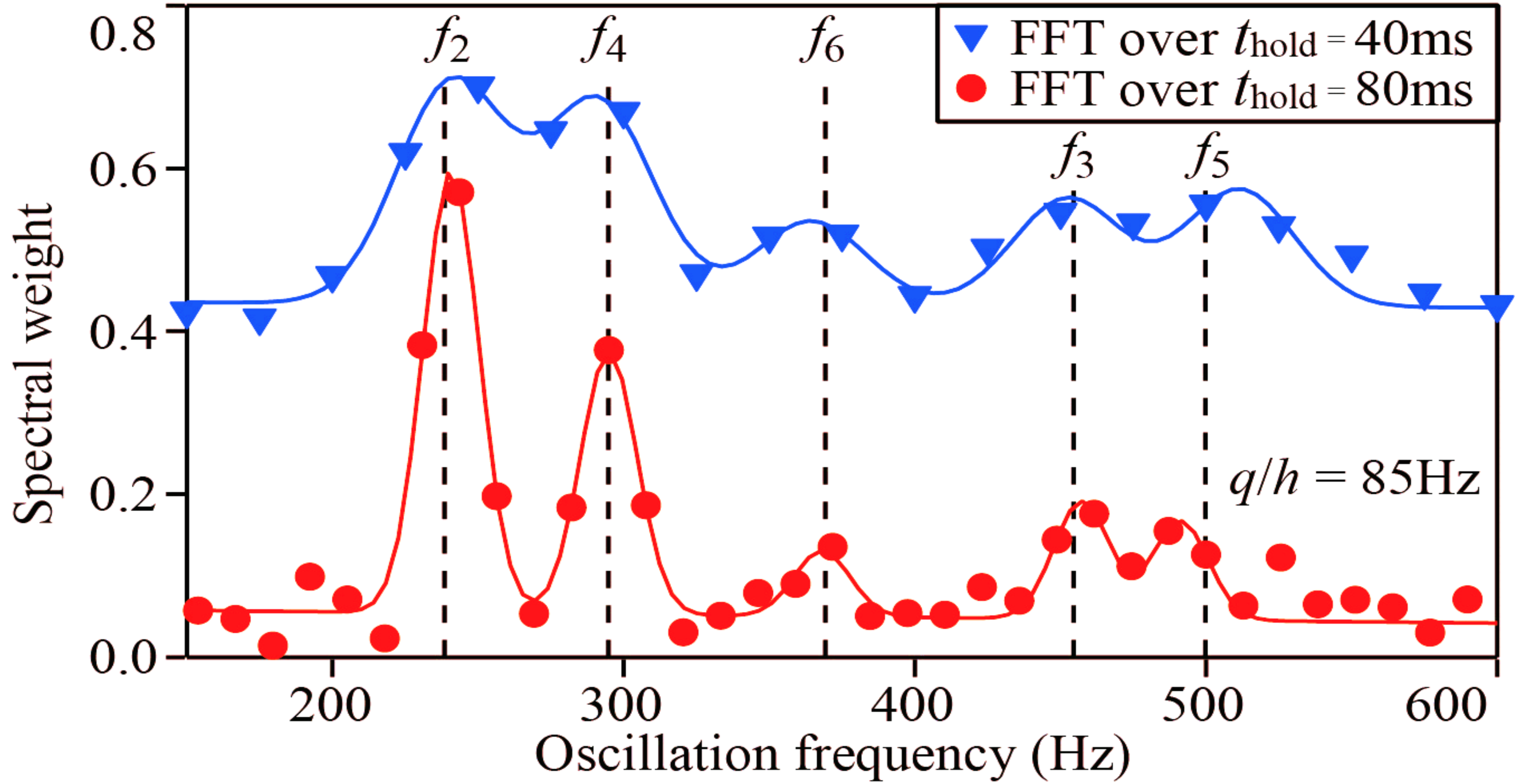

By dividing the area below the corresponding peak in a FFT spectrum by the spin oscillation amplitude, we can precisely determine χ_n (the fraction of atoms localized in lattice sites having ***n*** atoms)

Atom Number Distributions

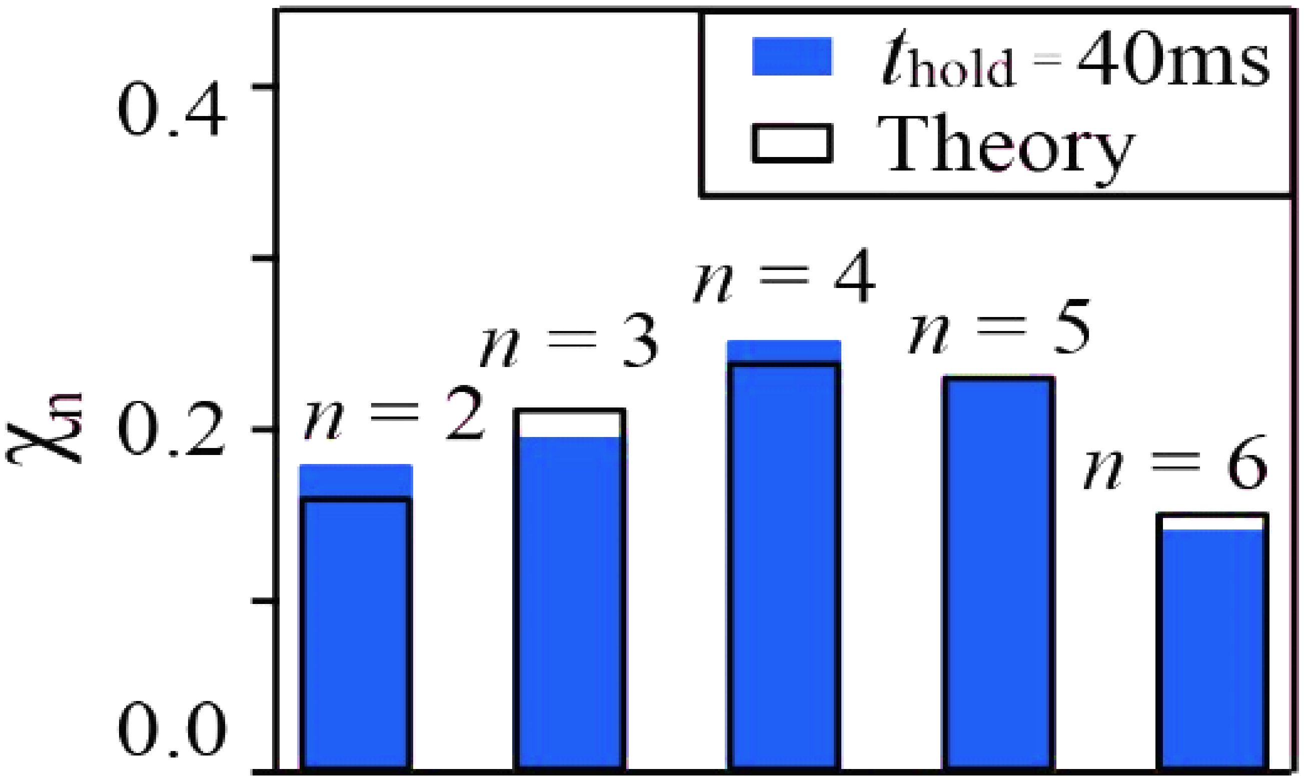

χ_n : the fraction of atoms localized in lattice sites having $\boldsymbol{n}$ atoms

- Good agreement with predictions based on the simplified spinor Bose-Hubbard model

Effects of Varying Lattice Quench Speed

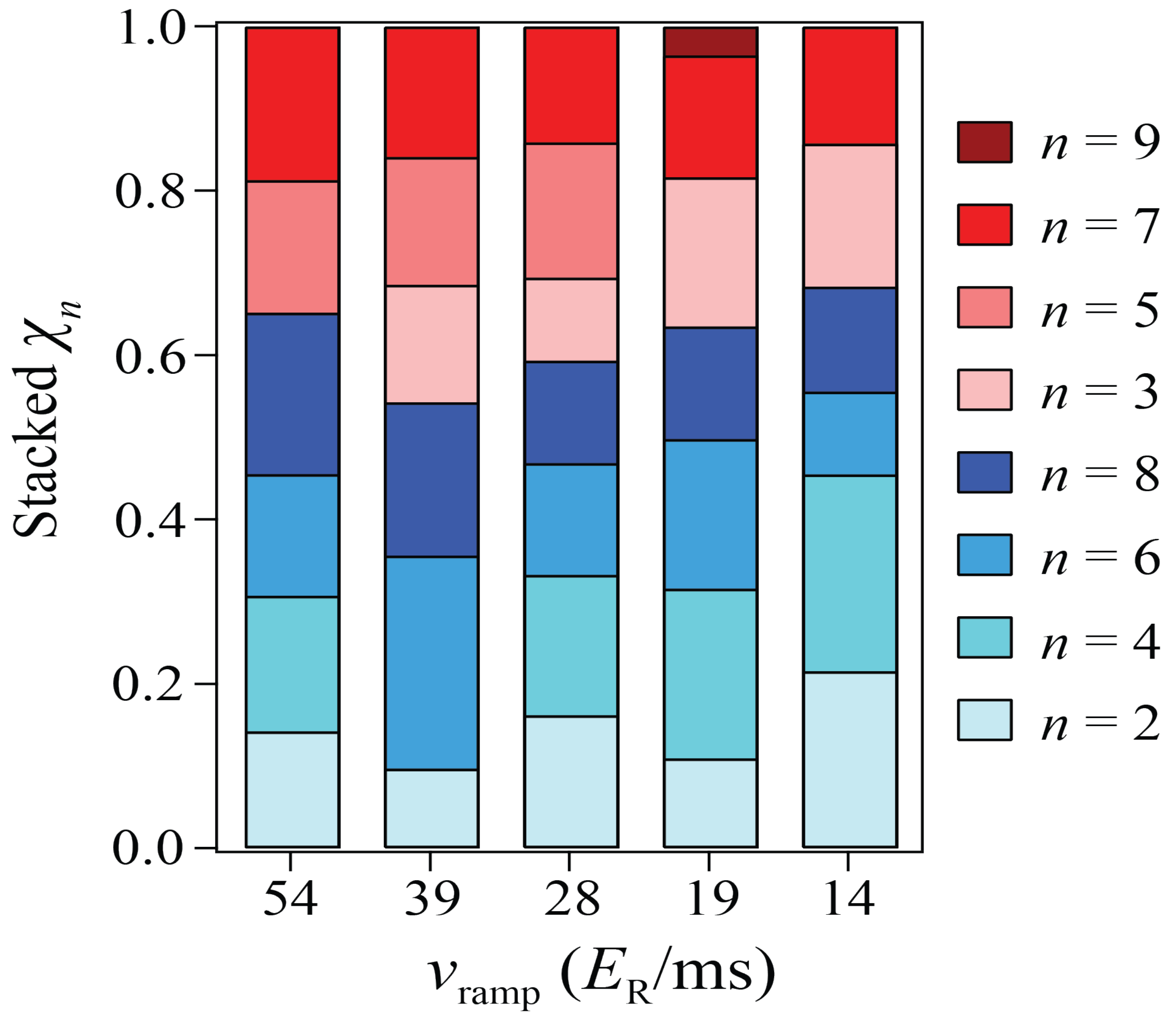

Shades of blue represent ***even* occupation number *n*** per lattice site, shades of red represent ***odd* occupation number *n*** per lattice site, with the shades getting darker as ***n*** increases

Revealing spatial dynamics of 3D lattice systems

Lattice site resolved imaging of 3D systems is very challenge
while 1D and 2D systems have been detected by quantum gas microscopy

The observed atom number distributions can be combined with the predicted wedding cake structure to reveal the spatial dynamics of 3D systems

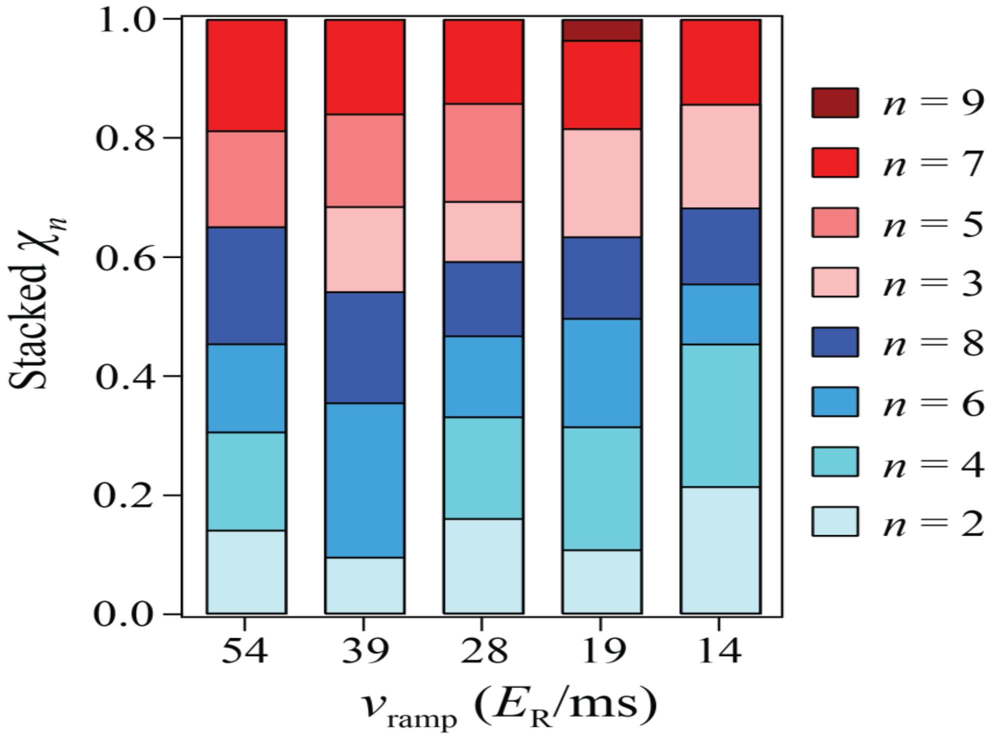

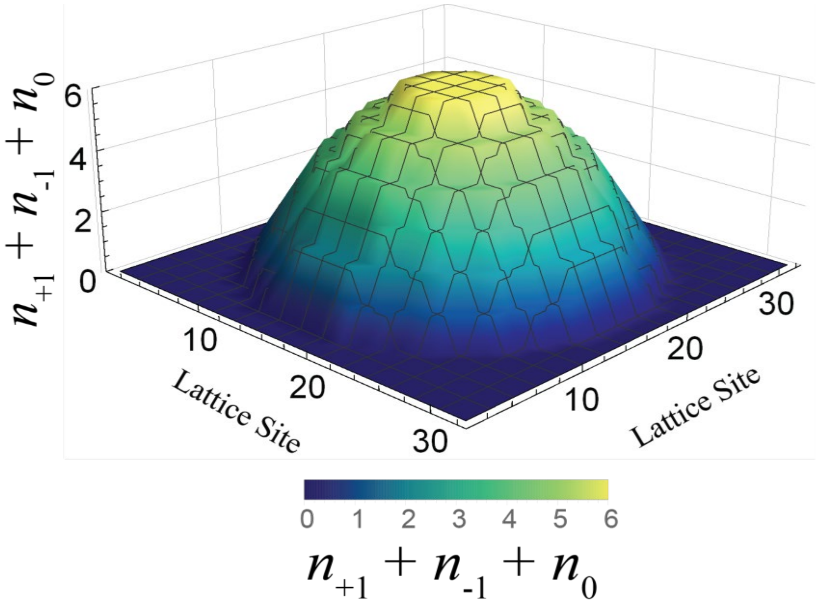

- Plateaus with integer ***n***
- Higher ***n*** towards the center of the trap
- Lower ***n*** towards the edges

Revealing spatial dynamics of 3D lattice systems

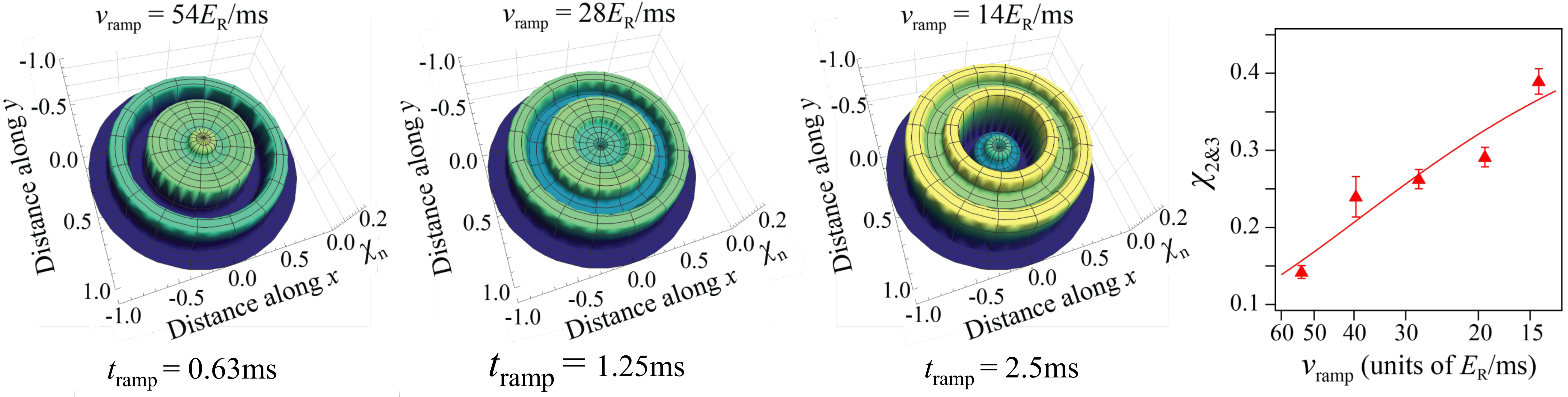

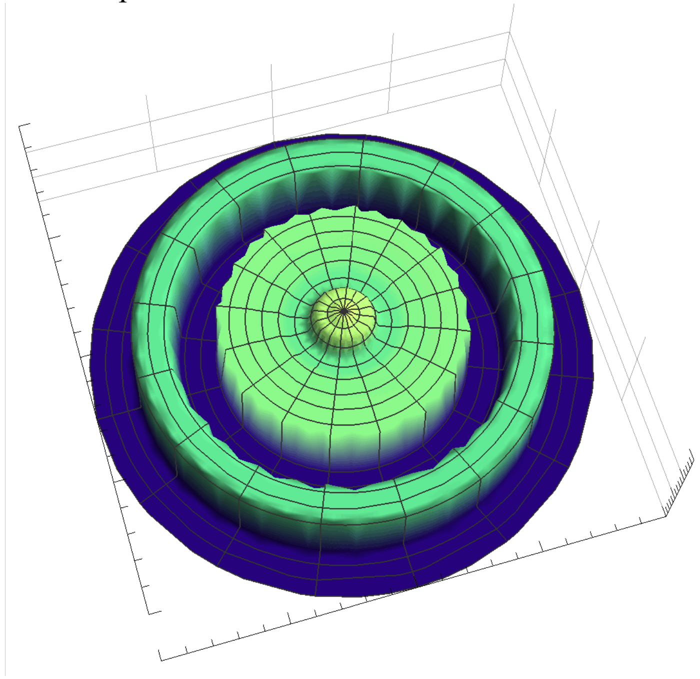

Slower lattice quenches allow atoms initially located in the trap center to have more time to flow to the trap boundaries resulting in a higher proportion of atoms in sites with lower occupation numbers.

This indirect imaging of spatial dynamics in 3D systems is useful, because direct imaging methods (e.g., quantum gas microscopy) are realized only in 1D and 2D systems.

Quantum critical dynamics of Superfluid to Mott-Insulator transitions

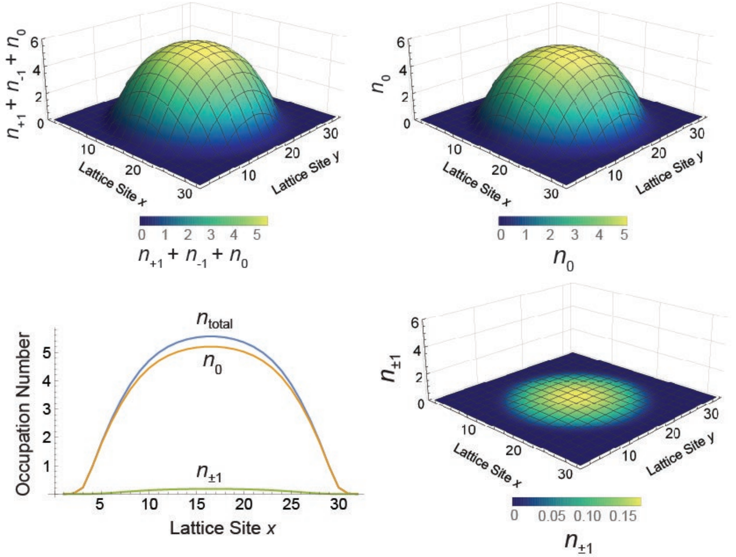

Fast Lattice Ramp

- Poissonian Density Distribution
- Minimal Spin -±1 Populations

Two good observables for the SF-MI phase transition:

- The SF order parameter
- Fractional population of spin-0 atoms

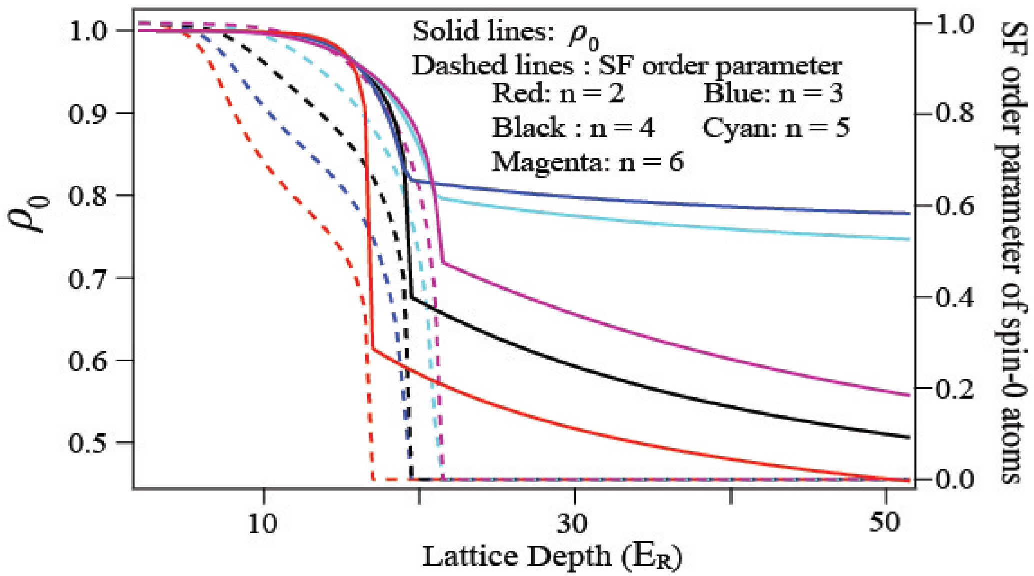

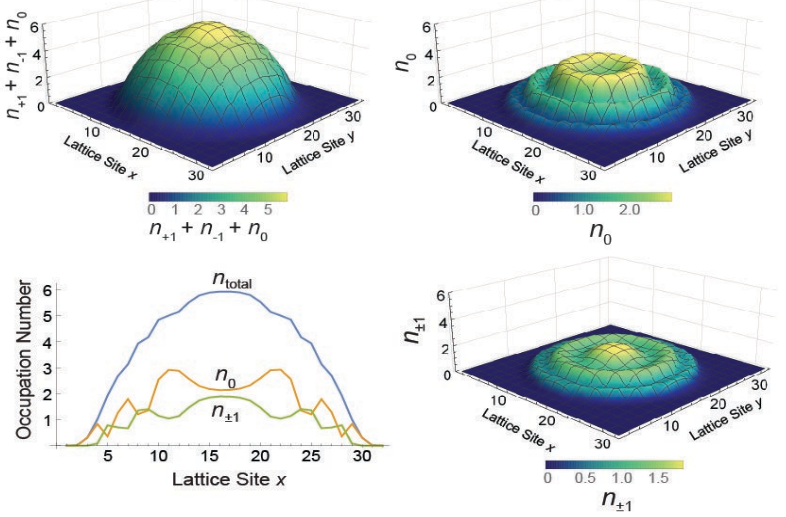

Slow Lattice Ramp

- Wedding Cake Density Distribution
- Relatively High Spin -±1 Population

Quantum critical dynamics probed via spin populations

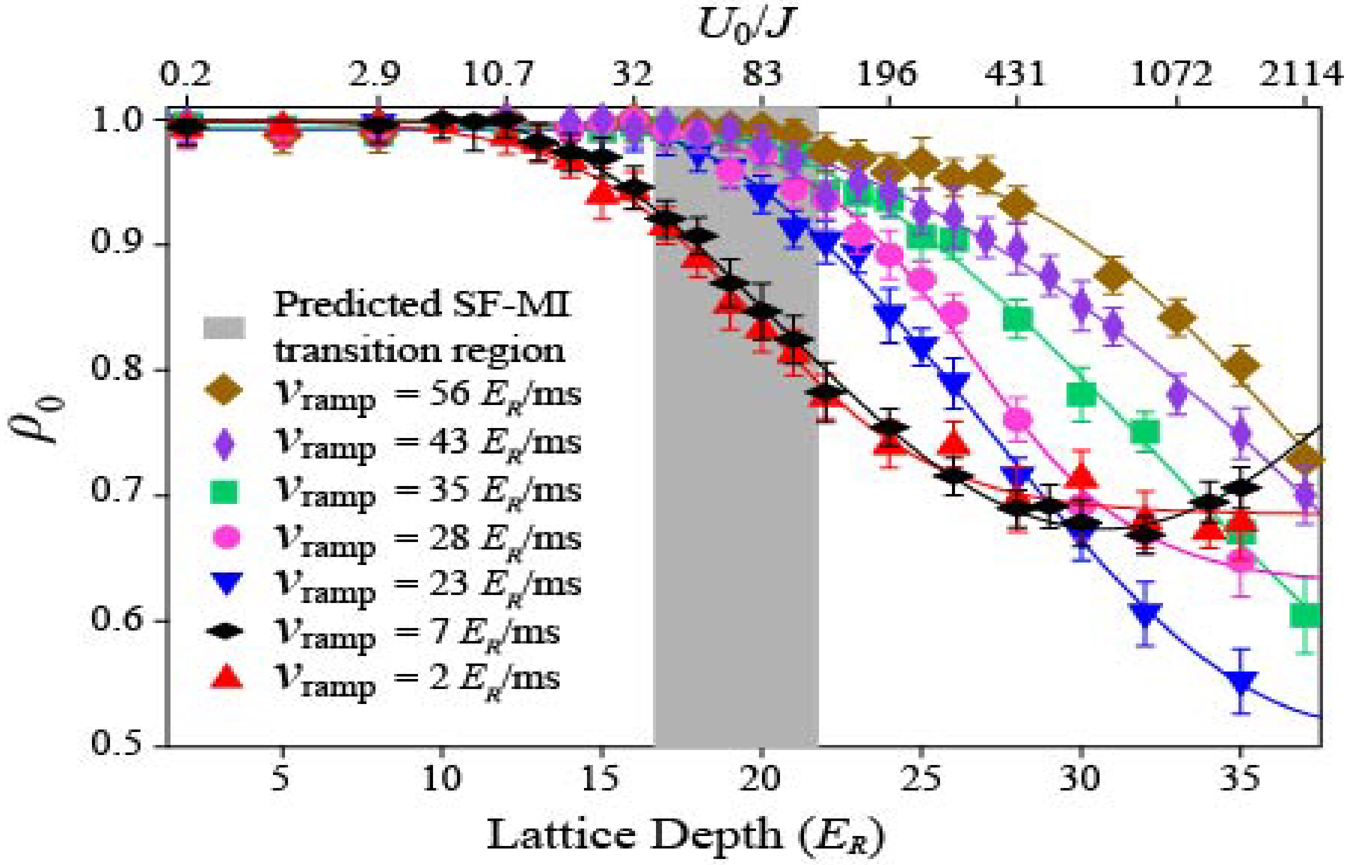

Experimental results

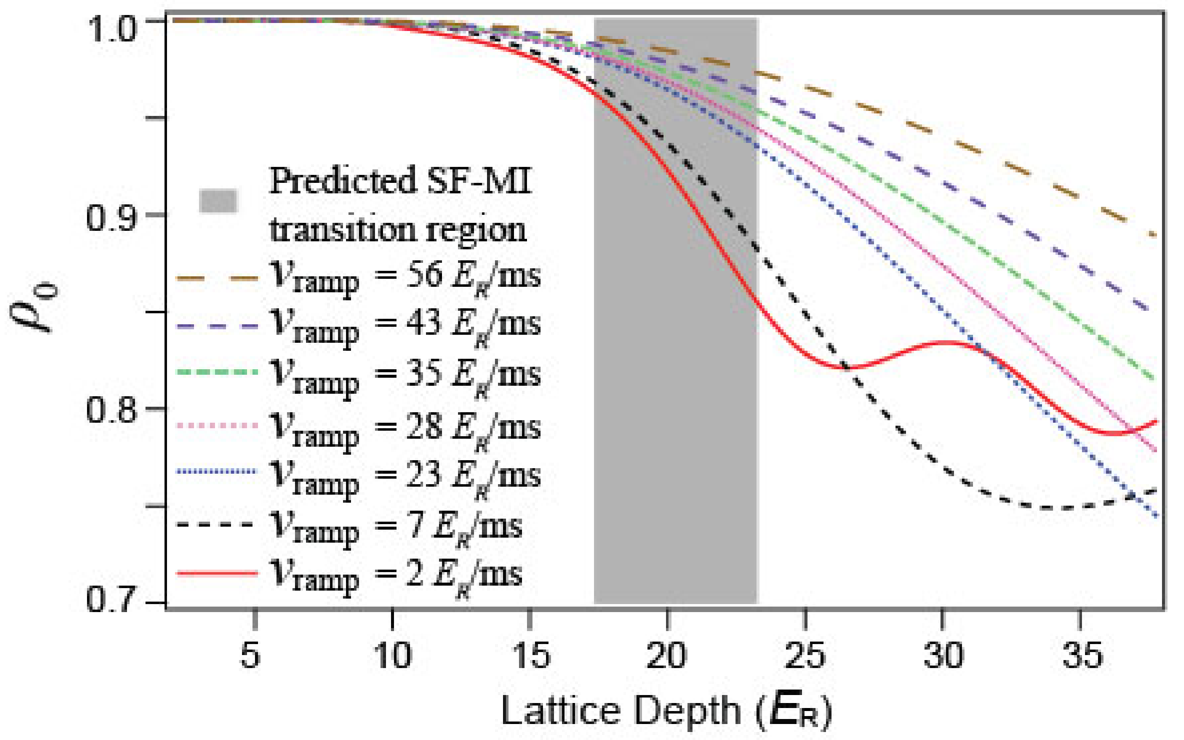

2D theoretical simulations

Quantum critical dynamics probed via the SF order parameter

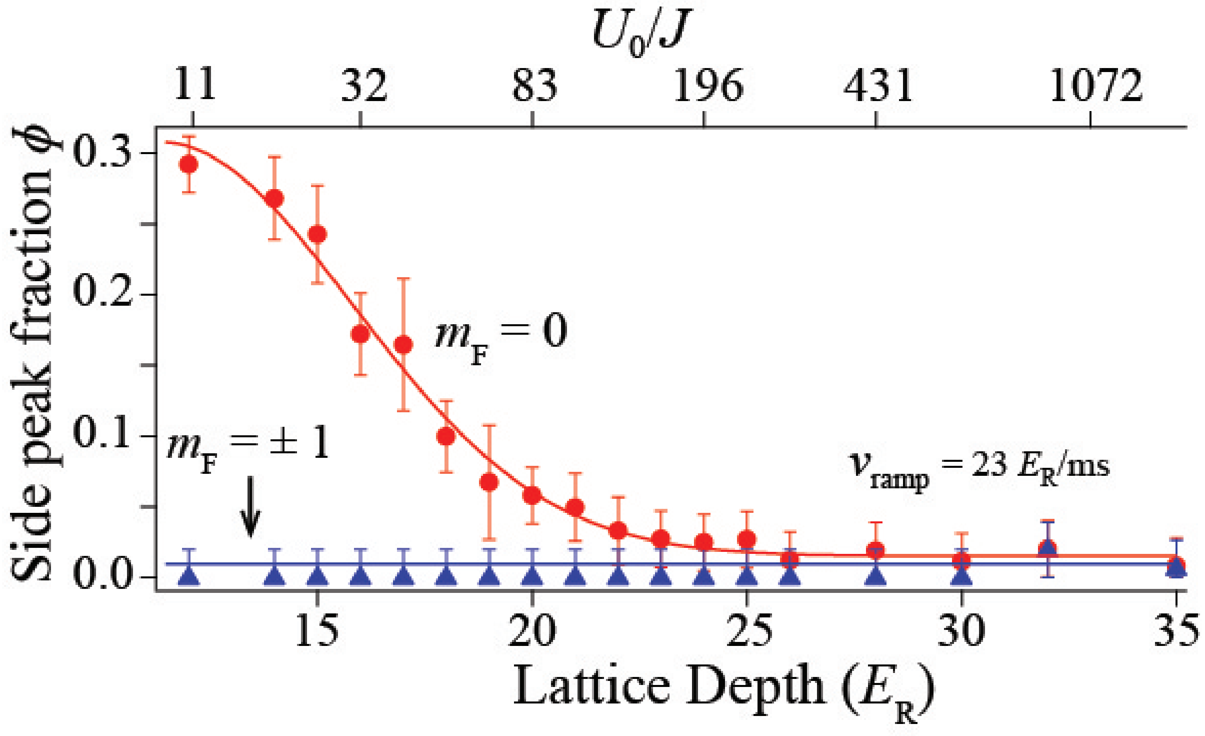

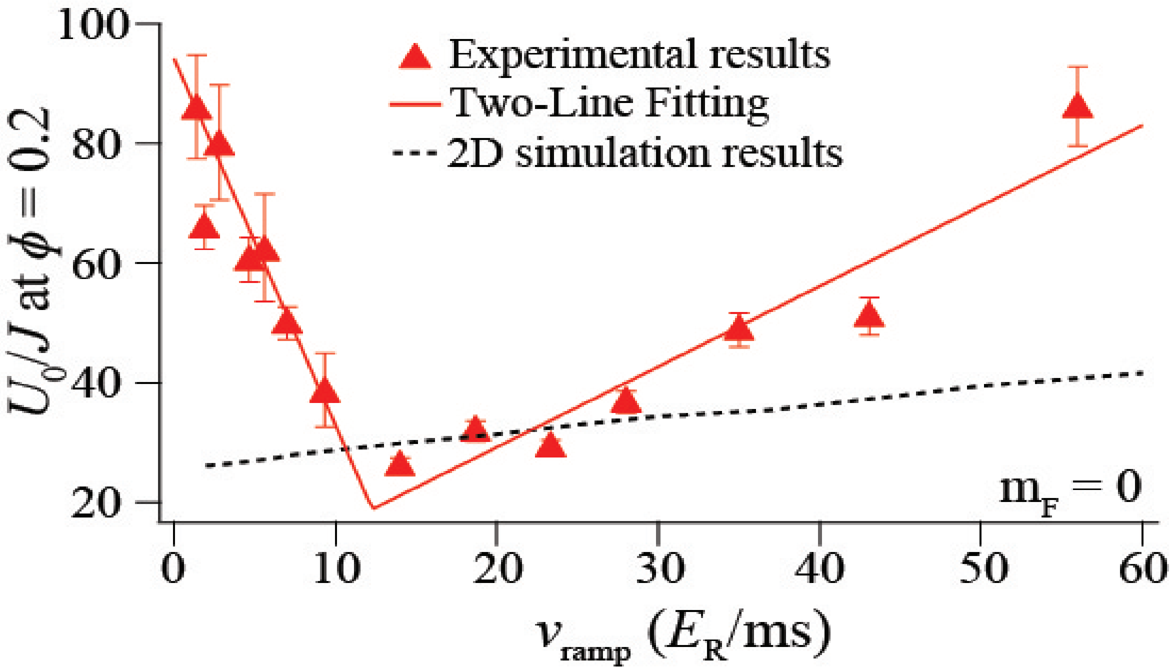

Large theory-experiment disagreements:
Theoretical studies of complicated 3D many-body systems are challenging due to limitations of existing numerical techniques so only 2D numerical simulation results are shown

Driven lattices: Engineering the dynamic phase diagram

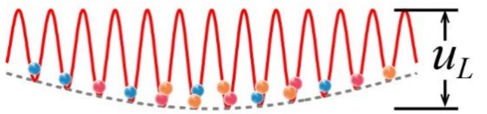

Adiabatically ramp up 1D optical lattice

RF pulses to prepare initial state

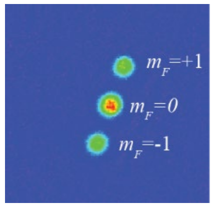

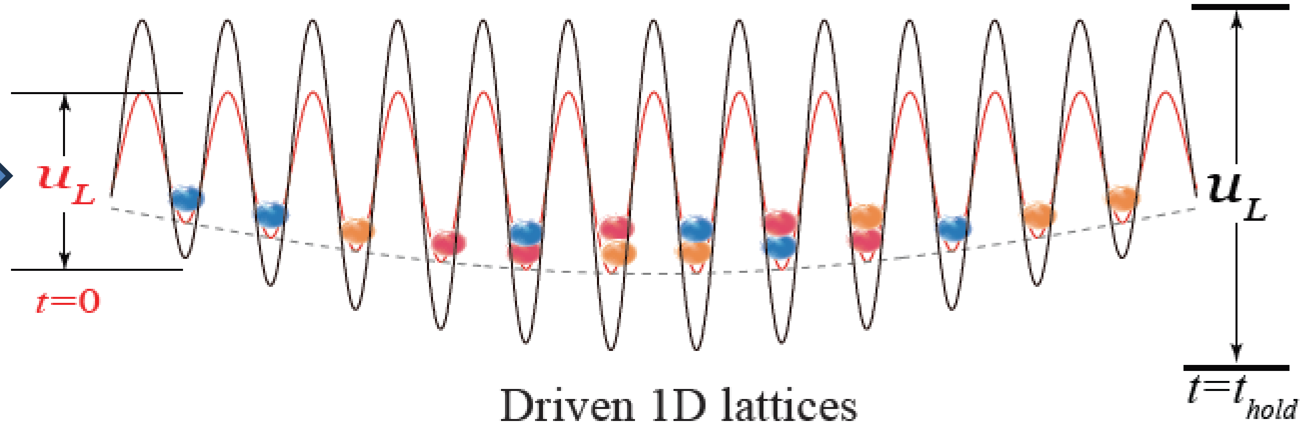

Driven 1D lattices

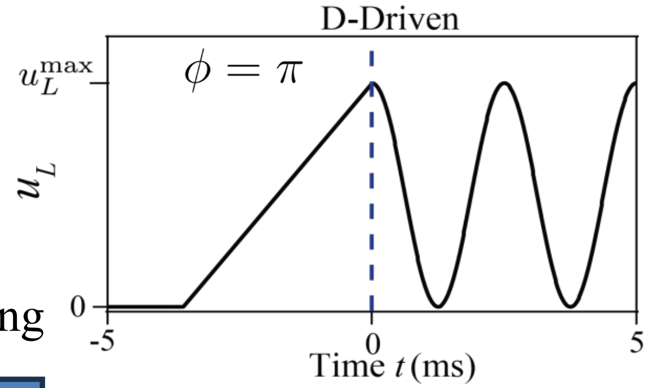

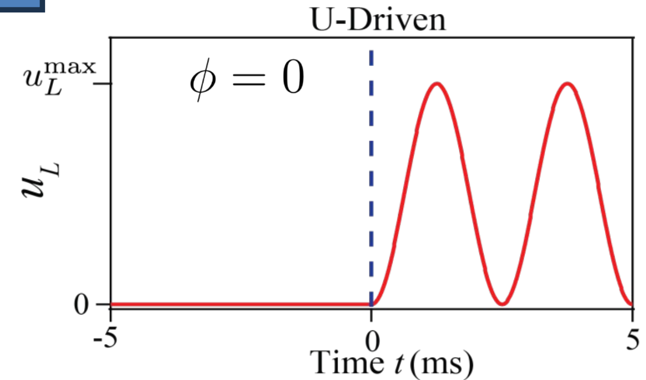

Sinusoidally modulate u_L at frequency f

$$u_L(t) = (u_L^{\max}/2)[1 + \cos(2\pi f t - \phi)]$$

Release for Imaging

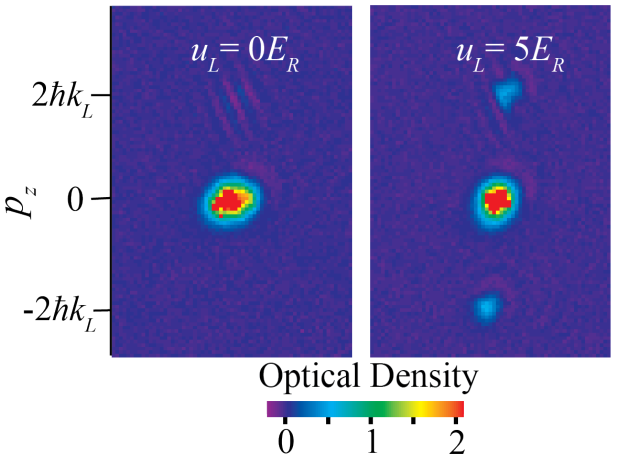

Driven lattices: Engineering the dynamic phase diagram

Dynamic SMA model: $c_2(t) = \mathcal{G}_0 + \sum_{j=1}^{\infty} \mathcal{G}_j \cos(j2\pi f t - \Phi_j)$

$\mathcal{G}_0$- Spin-preserving interaction
$\mathcal{G}_j$- Spin-changing interaction

$$\hat{H}_{\mathrm{mf},j} = \boxed{q_{\mathrm{eff},j}}(1-\rho_0) + \boxed{\mathcal{G}_0}\rho_0(1-\rho_0) + \frac{\boxed{\mathcal{G}_j}}{2}\rho_0\sqrt{(1-\rho_0)^2 - M^2}\cos(\boxed{\theta_{\mathrm{eff}}})$$

Interactions Tuned by Amplitude of Driven Lattice

$$q_{\mathrm{eff},j} = q - jhf/2$$

Effective q Controlled by Frequency of Driven Lattice

$$\theta_{\mathrm{eff},j} = \theta + \Phi_j$$

Effective Phase Controlled by Phase of Driven Lattices

Free space: $\hat{H}_{\mathrm{mf}} = q(1-\rho_0) + c_2\rho_0(1-\rho_0) + c_2\rho_0\sqrt{(1-\rho_0)^2 - M^2}\cos(\theta)$

Driven lattices can simultaneously tune multiple key parameters of spinor physics with negligible heating and atom loss

New separatrices induced by driven lattices at higher q determined by the driven frequency f

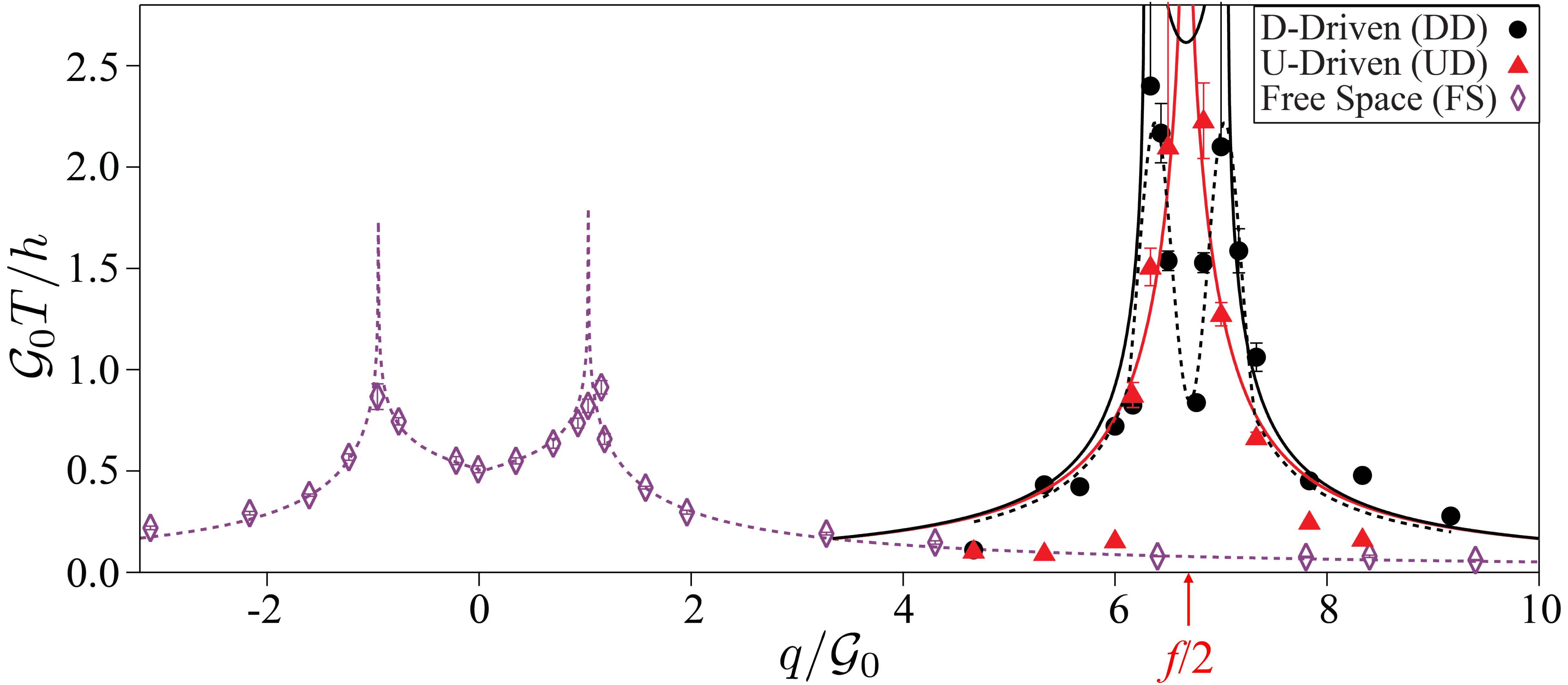

Solid lines are dSMA predictions

Additional separatrices induced by driven lattices at higher harmonics

Red: $q_{\mathrm{eff},1}/h = q/h - f/2$

Blue: $q_{\mathrm{eff},2}/h = q/h - f$

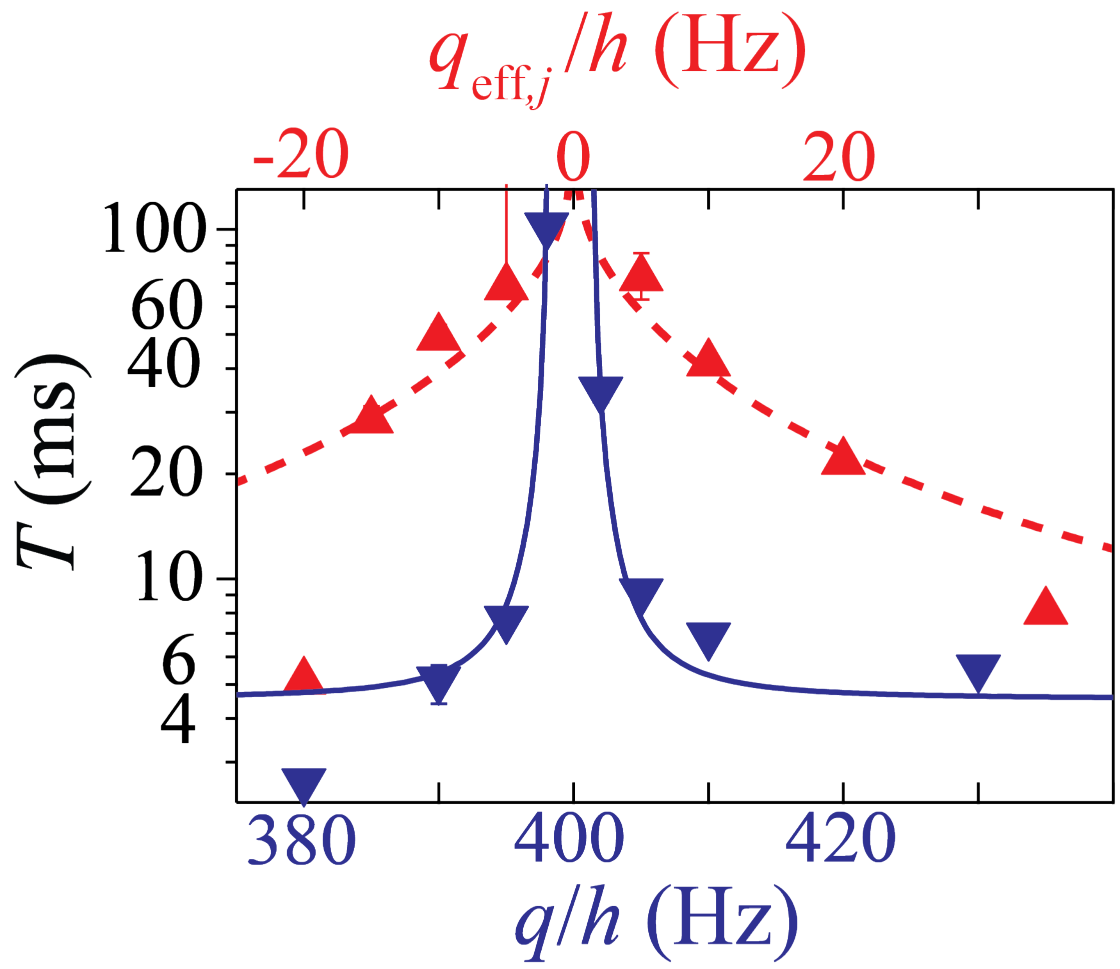

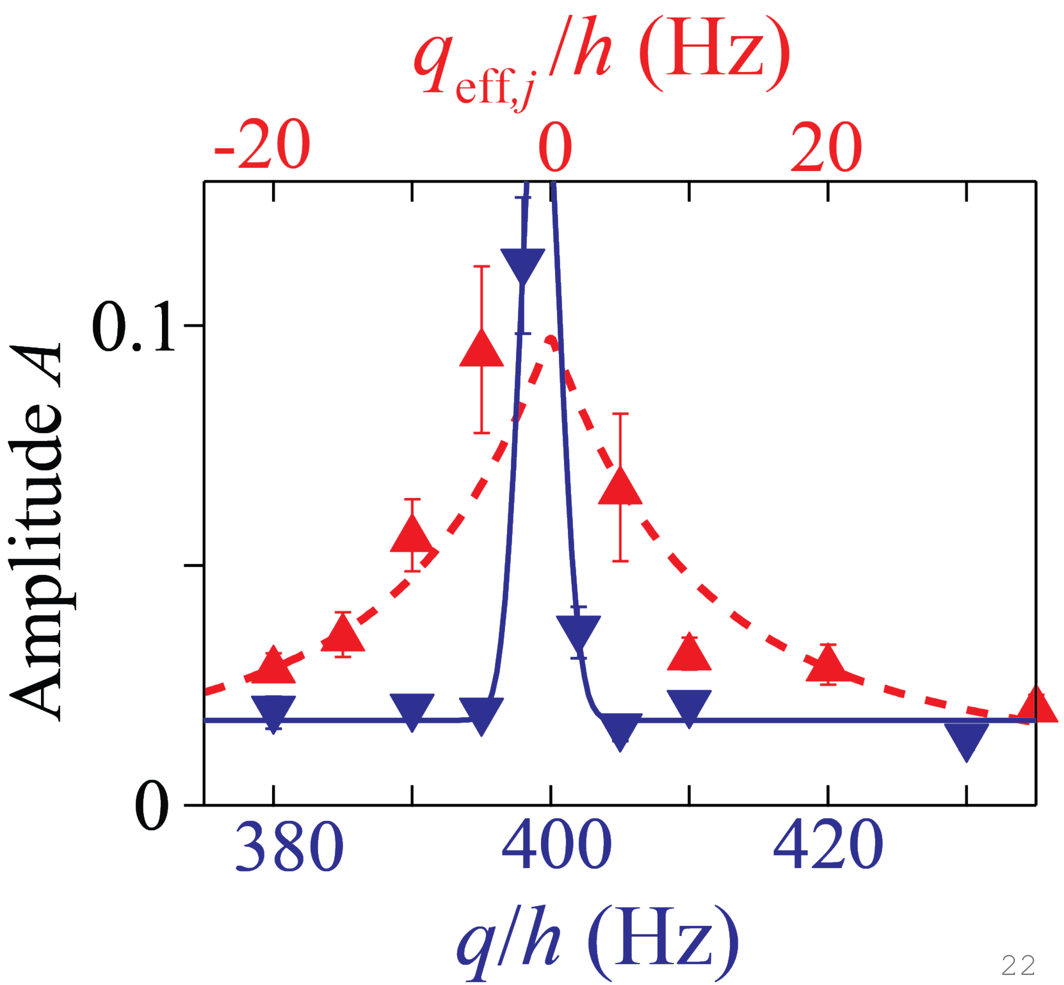

Coupling of spatial and spin degrees of freedom via moving lattices

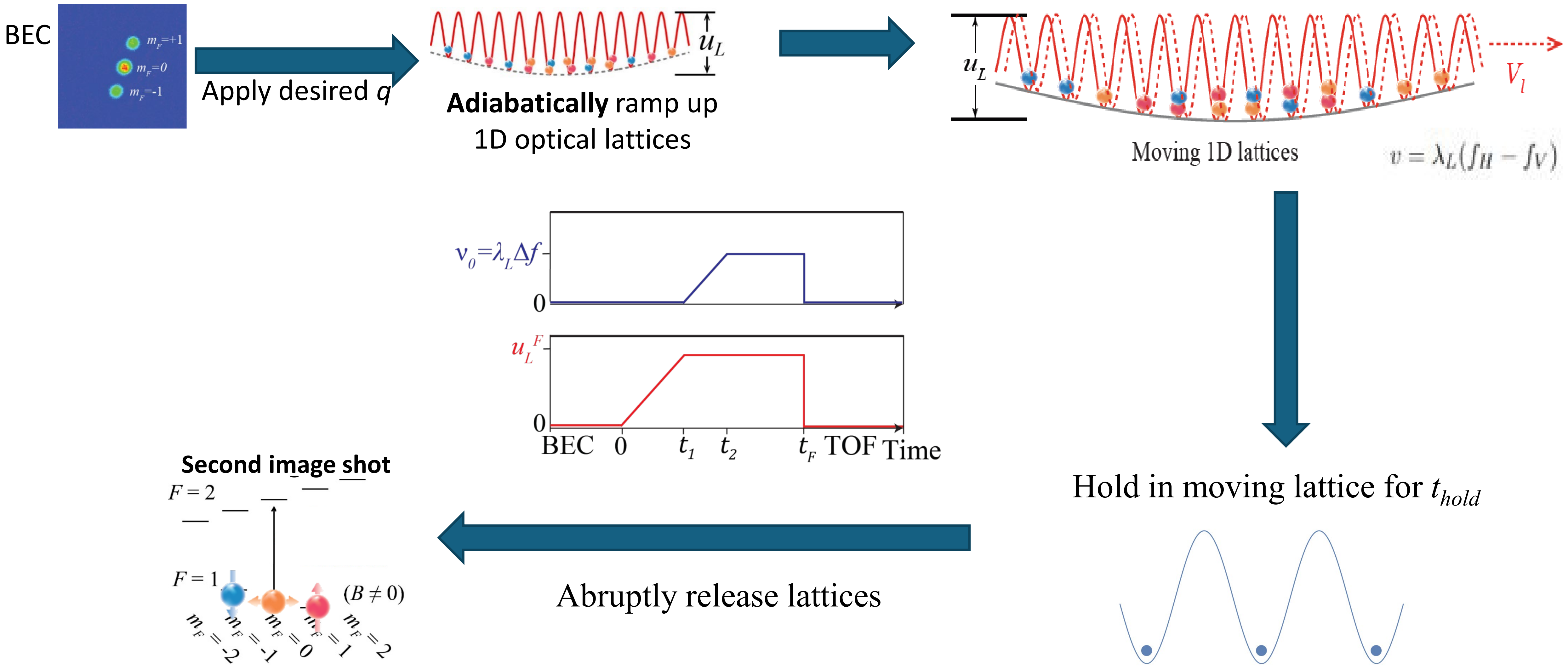

Coupling of spatial and spin degrees of freedom:

Violent spatial evolutions tune long-lived coherent spin dynamics

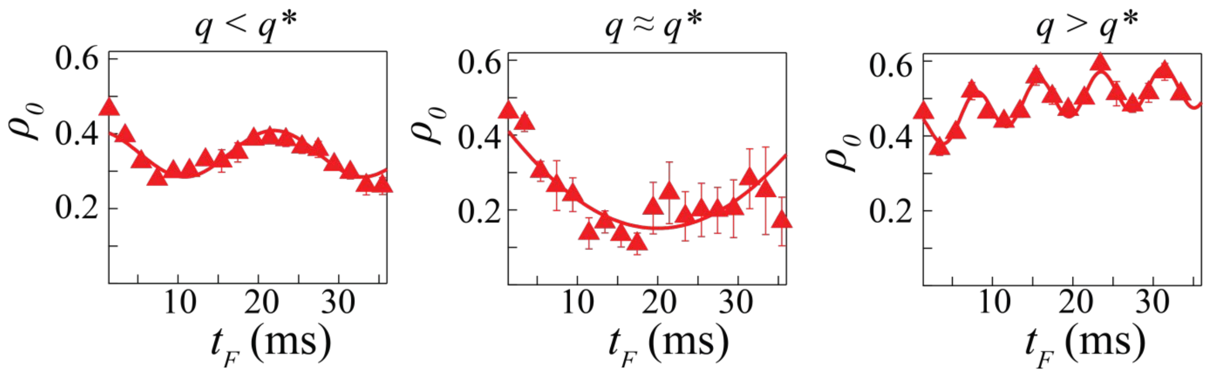

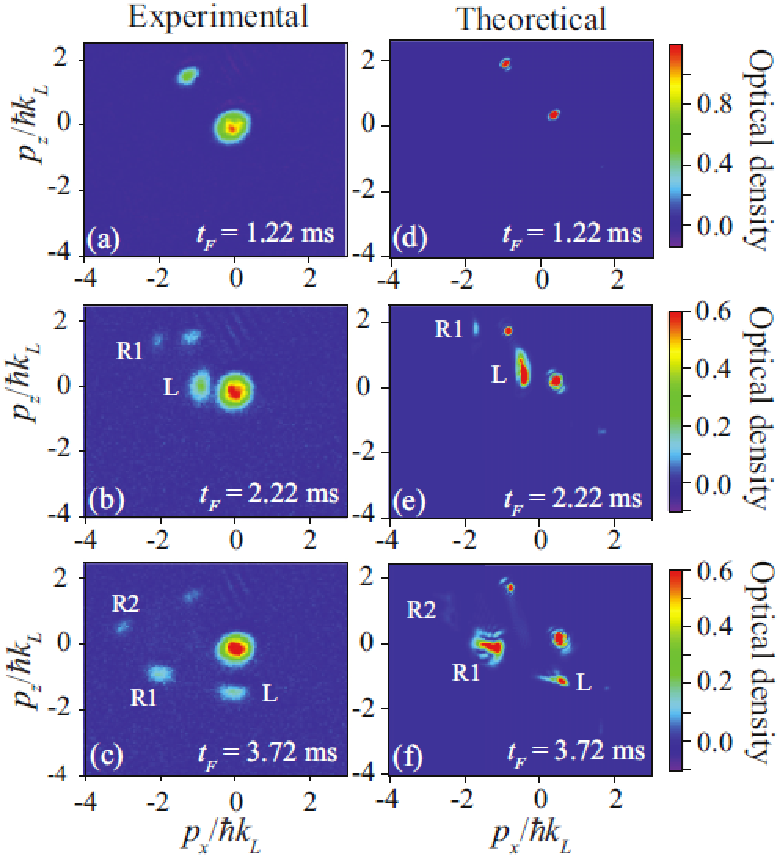

Time-of-flight snapshots of momentum distribution capture the emergence of violent spatial motion due to momentum kicks generated by the moving lattice and a skew shallow harmonic confinement.

$$\hat{H}_{\text{eff}}(t) = \frac{c_2(t)}{2N}\hat{\mathbf{S}} \cdot \hat{\mathbf{S}} + q(\hat{n}_1 + \hat{n}_{-1}).$$

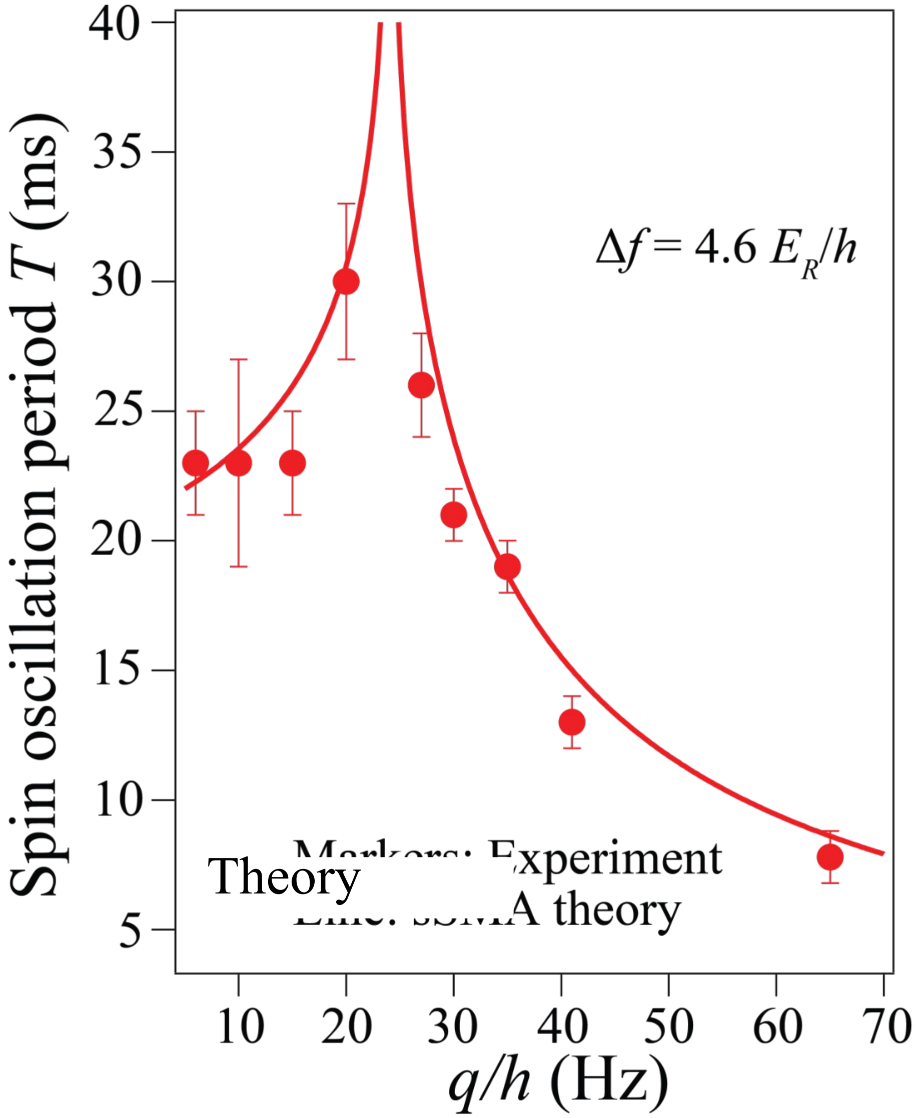

Quantum scars in spinor gases

- Quantum states thermalize in accordance with eigenstate thermalization hypothesis **(ETH)**: eigenstate expectation values vary smoothly with energy [J. M. Deutsch, PRA 43, 2046 (1991).]
- Mechanisms for avoiding thermalization: integrability, many-body localization, quantum many-body scars, Hilbert-space fragmentation, and quantum scars, with potential applications to quantum transport, quantum metrology, and quantum information storage.
- Weak ETH breaking: generic states obey ETH but a small subset of special states ("quantum many-body scars") do not. Can be associated with an integrable subspace of a non-integrable model.
- Spinor gases **uniquely positioned** to address both QMBS and quantum scars

F = 1 spinor BECs driven by weak spin-flopping fields

$$\hat{H}_{\mathrm{spin}} = h\left[\underbrace{\frac{c_2}{N}\sum_{i<j}\hat{\mathbf{s}}_i\cdot\hat{\mathbf{s}}_j + \sum_i\left(p_z\hat{s}_{z,i} + q_z s_{z,i}^2\right.}_{\text{Integrable}}\underbrace{\left. + \mathbf{p}_\perp\cdot\hat{\mathbf{s}}_{\perp,i}\right)}_{\text{Integrability Breaking}}\right]$$

Observation of QMBS in Spinor BECs

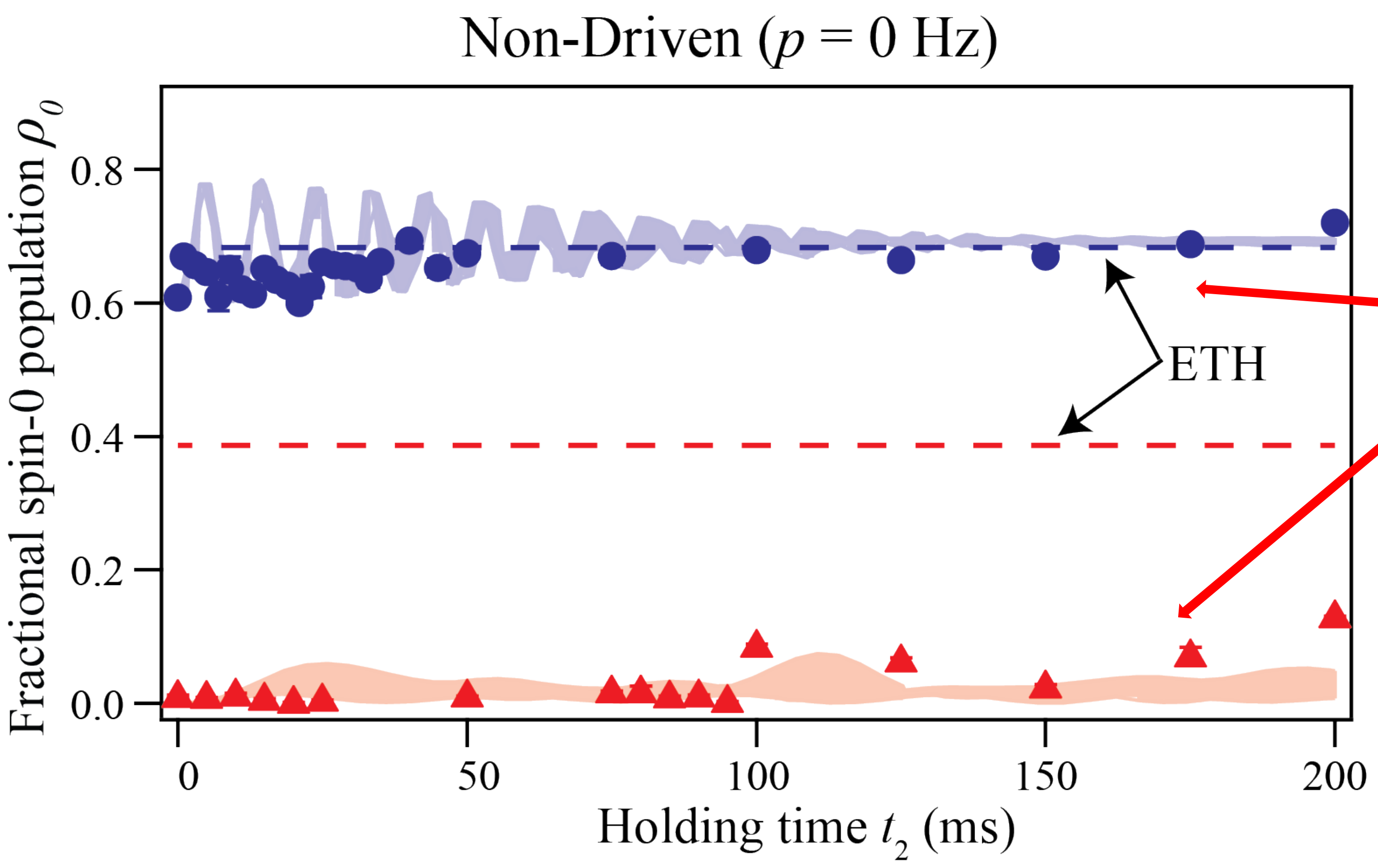

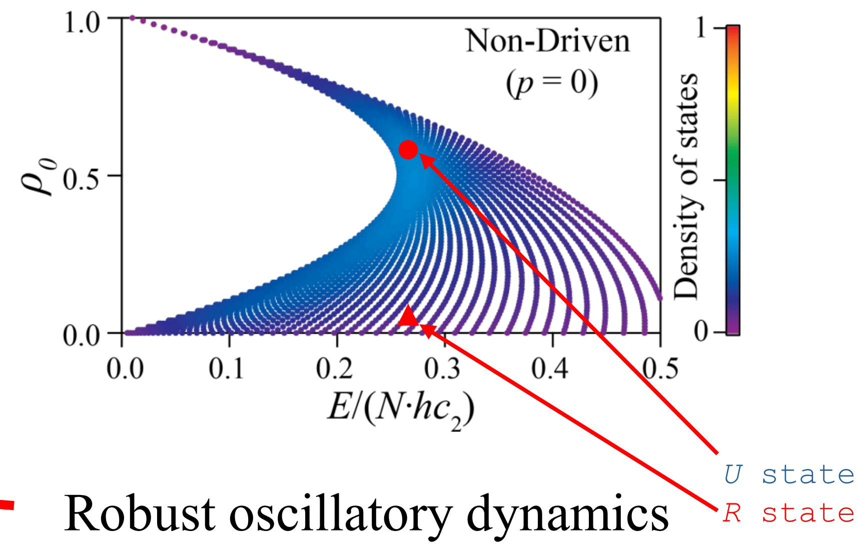

Robust oscillatory dynamics that don't necessarily thermalize to the ETH prediction

Blue (Red): U (R) states

Shaded Region: SMA model

$$\hat{H}_{\text{spin}} = h\left[\frac{c_2}{N}\sum_{i<j}\hat{\mathbf{s}}_i\cdot\hat{\mathbf{s}}_j + \sum_i (p_z\hat{s}_{z,i} + q_z s_{z,i}^2 + \mathbf{p}_\perp\cdot\hat{\mathbf{s}}_{\perp,i})\right]$$

Observation of QMBS in Spinor BECs

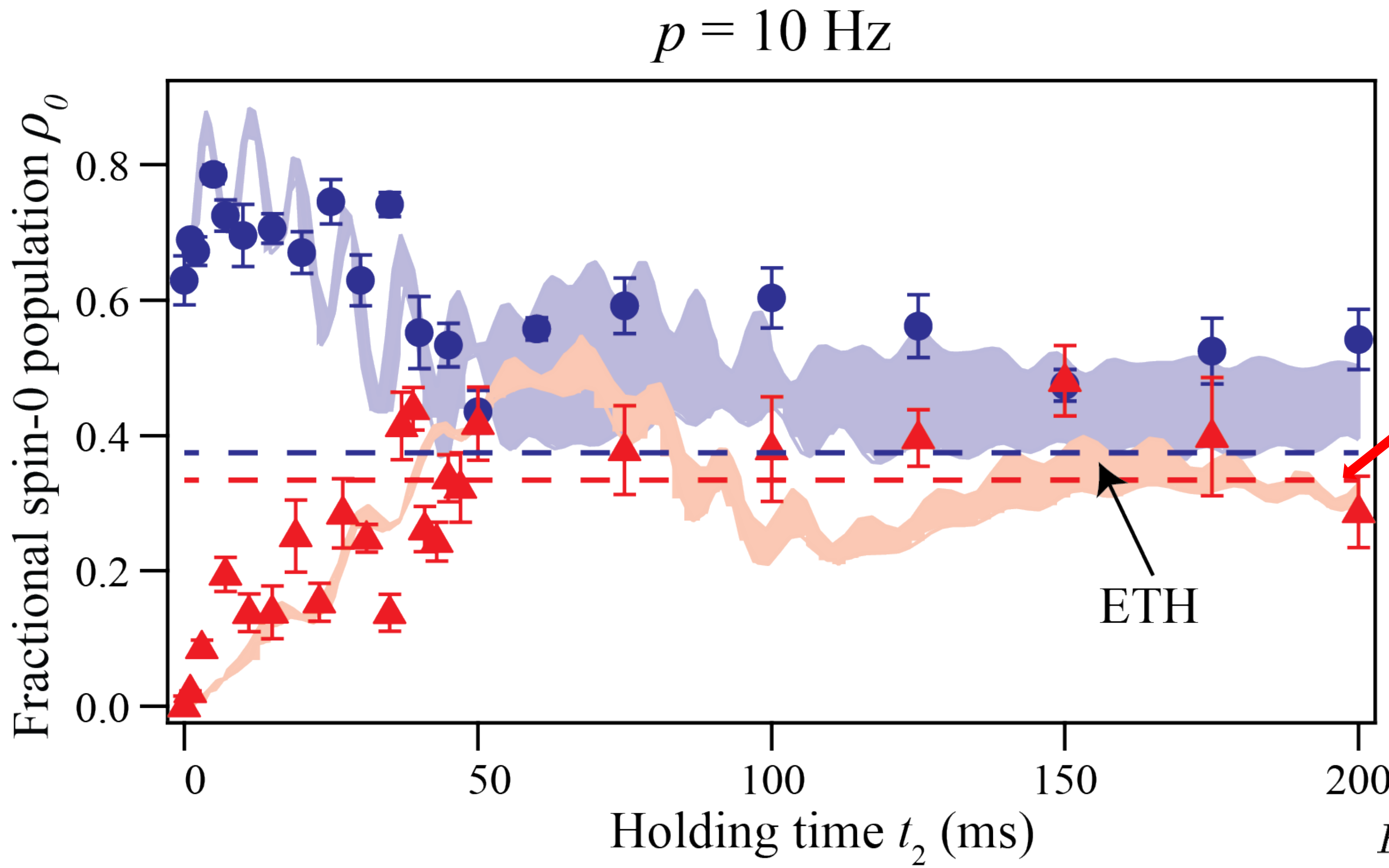

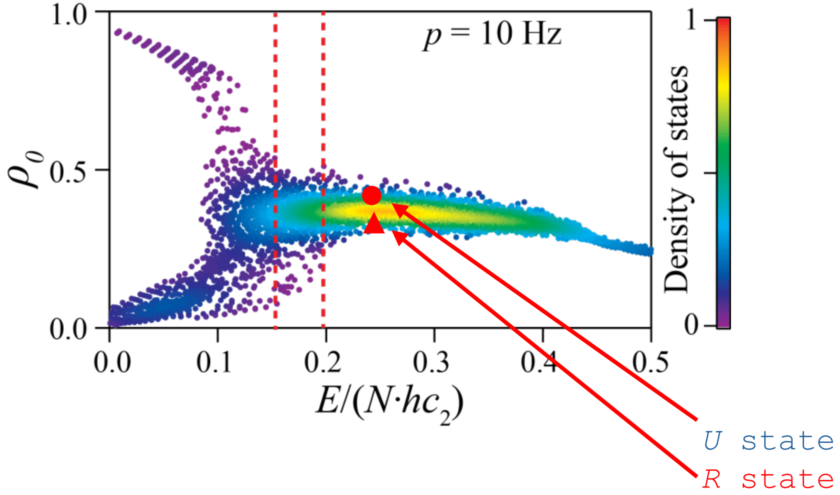

As p increases, the *R* state begins to thermalize and the dynamics start to overlap

Blue (Red): *U* (*R*) states
Shaded Region:SMA model

$$\hat{H}_{\text{spin}} = h\left[\frac{c_2}{N}\sum_{i<j}\hat{\mathbf{s}}_i\cdot\hat{\mathbf{s}}_j + \sum_i (p_z\hat{s}_{z,i} + q_z s_{z,i}^2 + \mathbf{p}_\perp\cdot\hat{\mathbf{s}}_{\perp,i})\right]$$

Conclusion

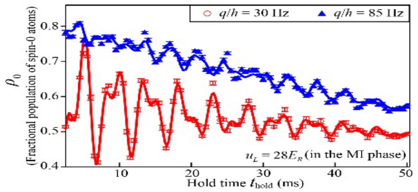

- In observed few-body nonequilibrium dynamics we can detect discrete energy signatures that reveal atom number distributions and allow us to deduce the spatial dynamics of 3D lattice systems.

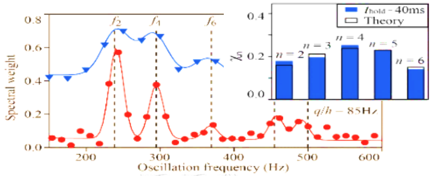

- We probe the quantum critical dynamics of the first-order SF-MI phase transitions by varying the rate at which our 3D lattice system is quenched across the transition.

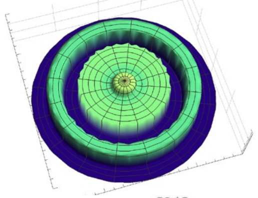

- By sinusoidally modulating the lattice depth of a 1D optical lattice, we engineer dynamical phase diagrams and demonstrate the capability to tune the key parameters that determine spinor physics using parameters of the driven lattice.

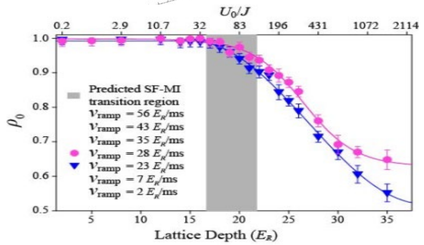

- We observe coherent spin dynamics in a spinor system that is subject to violent spatial dynamics. These spin dynamics appear to be well described by an SMA model demonstrating a surprising robustness of the approximation so long as all spin components share the same time dependent spatial mode.

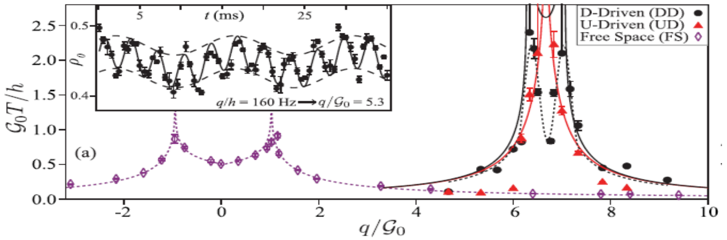

- Using weak spin-flopping fields, we break the integrability of the spin-1 spinor BEC model enabling the detection of quantum many-body scars in a scarred classical phase space.

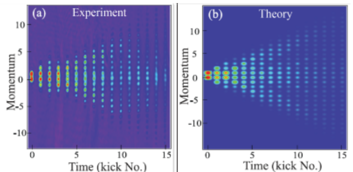

- We demonstrate a momentum space quantum walk which is predicted to be a first step in experimentally simulating all 1D and 2D topological phases classes.